Lubrication Effects on Surface Pitting and Scuffing in Gears - A Review

H. S. Cheng

Center for Engineering Tribology
Northwestern University

Evanston, IL 60208

Outline
of
Gear Lubrication Review

- Tribofailure Modes in Gears
- Lubrication Performance
- Mixed Lubrication Characteristics
    - $\bar{h}$ and h^* - Average and Asperity Film Thickness
    - $\bar{p}$ and p^* - Average and Asperity Pressure
    - $\bar{T}$ and T^* - Average and Asperity Contact Pressure
- Surface Fatigue Phenomenon
- Crack Initiation Modeling
- Crack Propagation Modeling
- Gear Teeth Contact Fatigue Life Modeling
- Scuffing Phenomenon
- Roller Simulation and Scuffing Experiments
- Scuffing Modeling
- Concluding Remarks

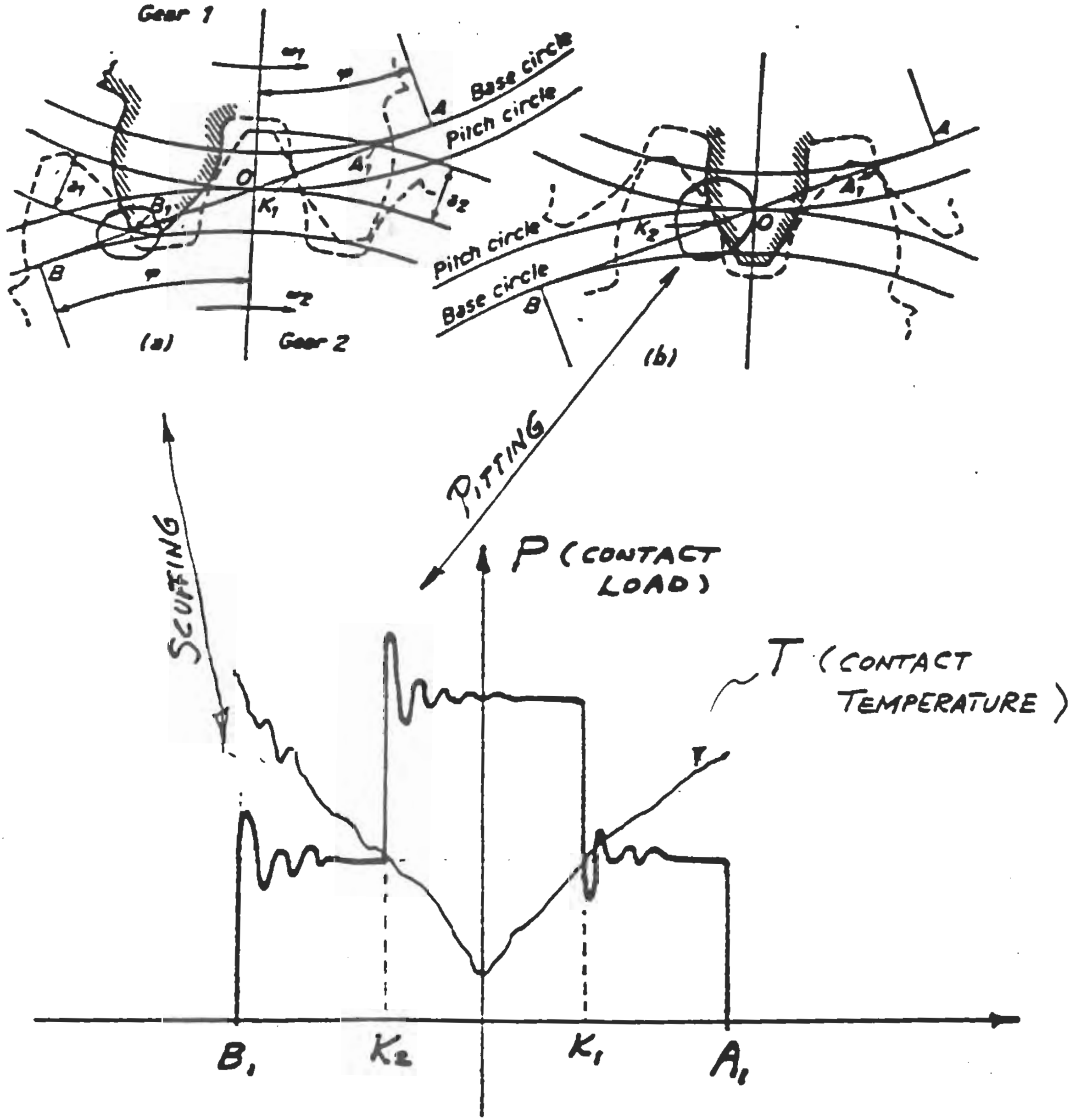
Gear 1
Base circle
Pitch circle
Gear 2
(a)
Pitch circle
Base circle
(b)
PITTING
SCUFFING
P (CONTACT LOAD)
T (CONTACT TEMPERATURE)
B1
K2
K1
A1

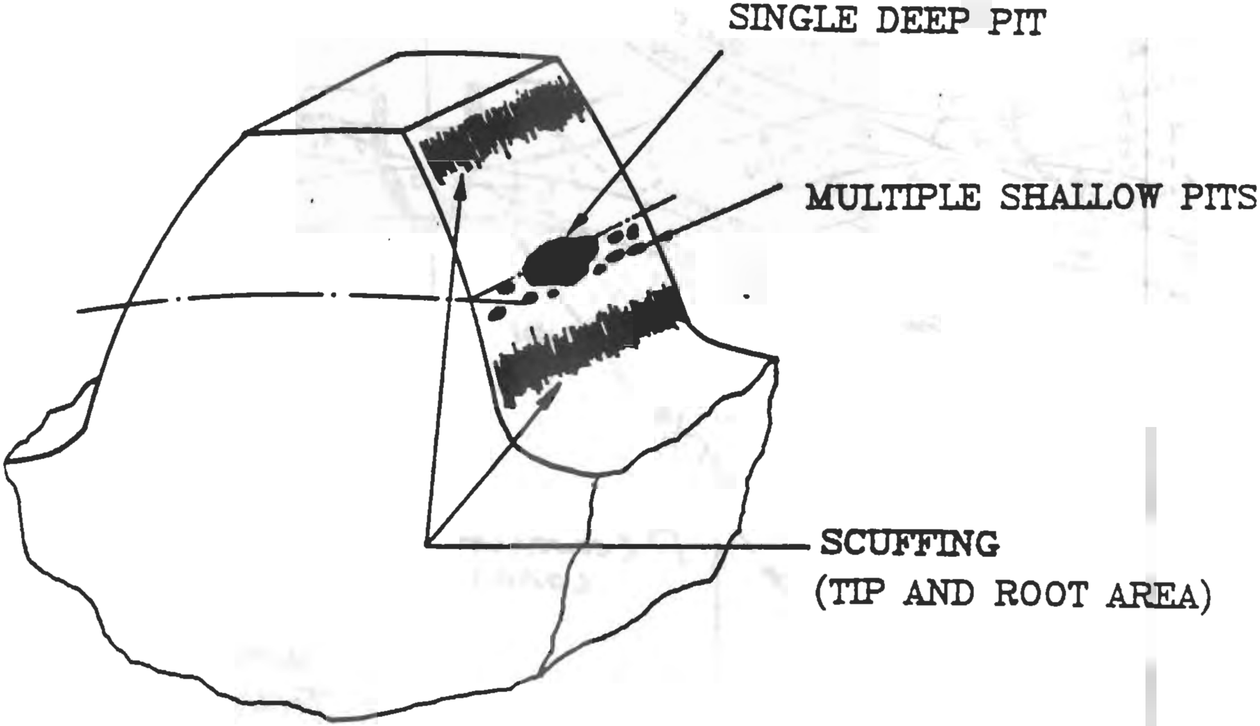
SINGLE DEEP PIT
MULTIPLE SHALLOW PITS
SCUFFING
(TIP AND ROOT AREA)

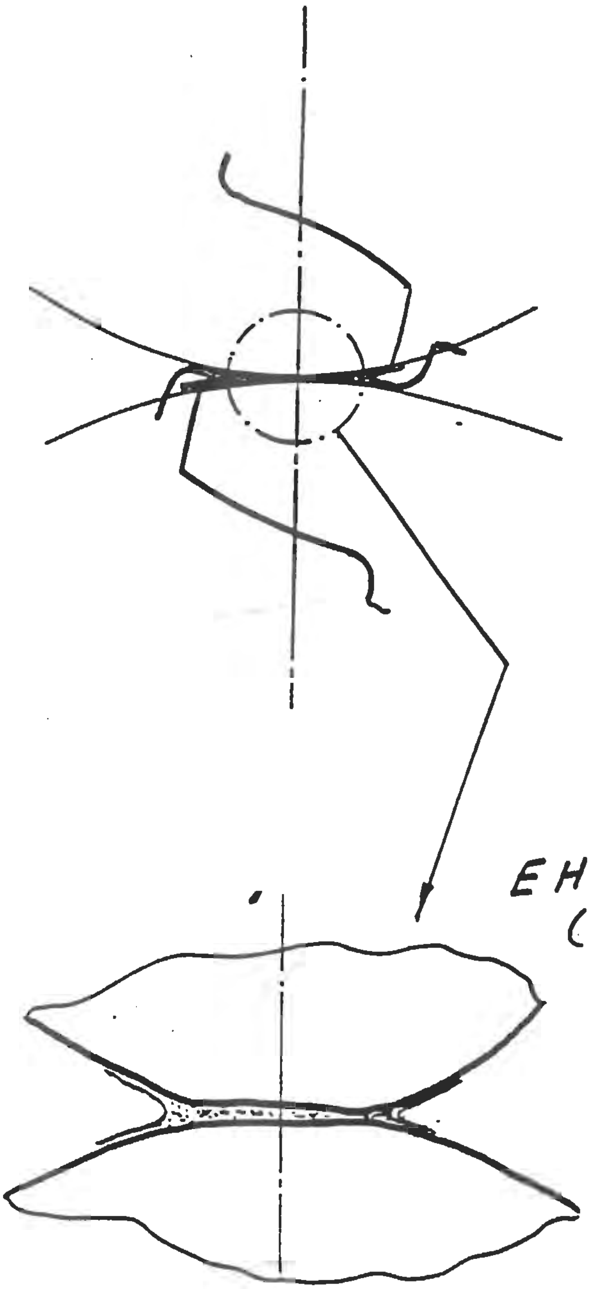

EHD
(ELASTOHYDRODYNAMIC LUBRICATION)

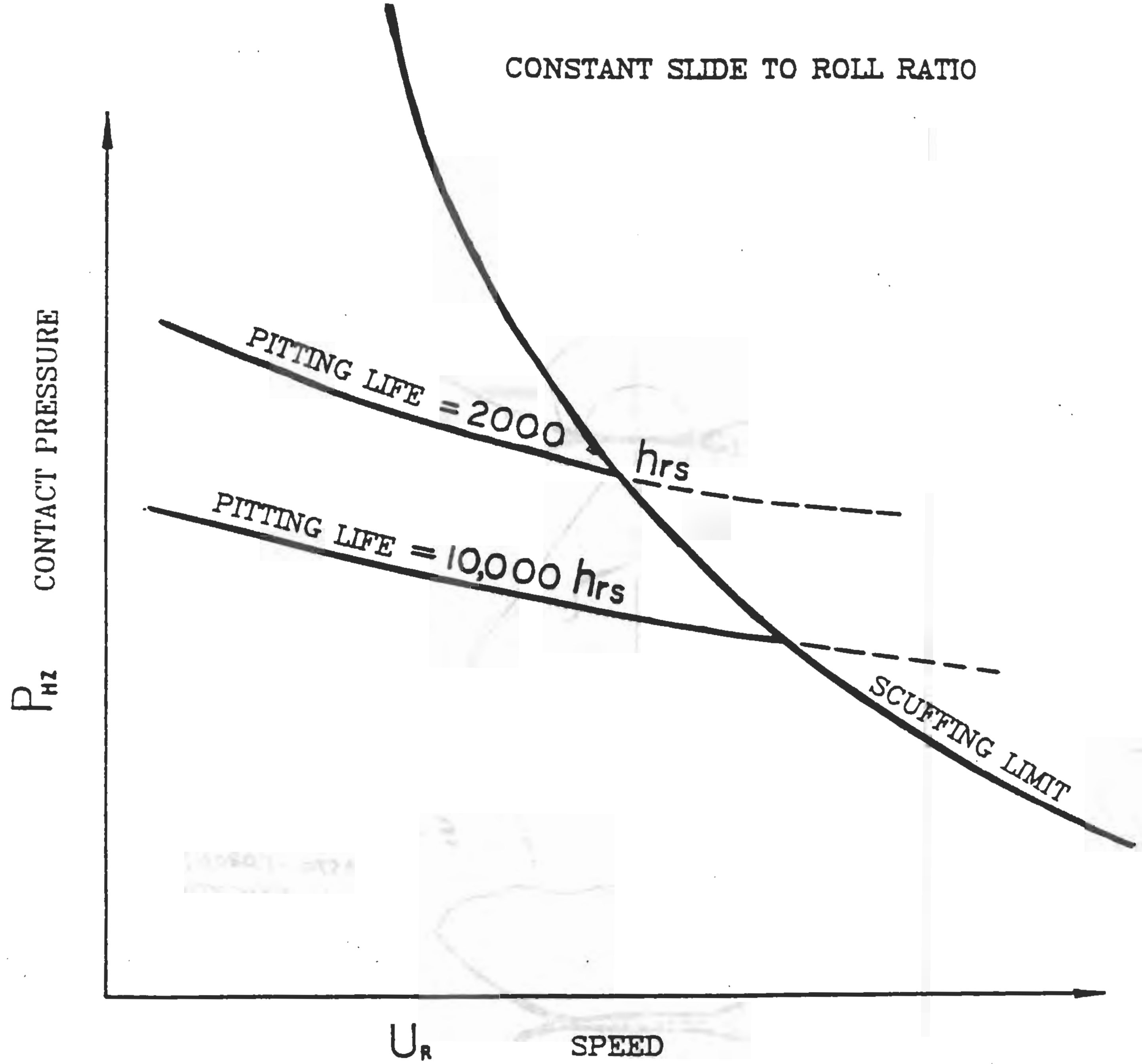

SIGNIFICANT EFFECTS :

ROLLING SPEED	INCLUSION
VISCOSITY	FIBER ORIENTATION
ROUGHNESS	
HARDNESS	

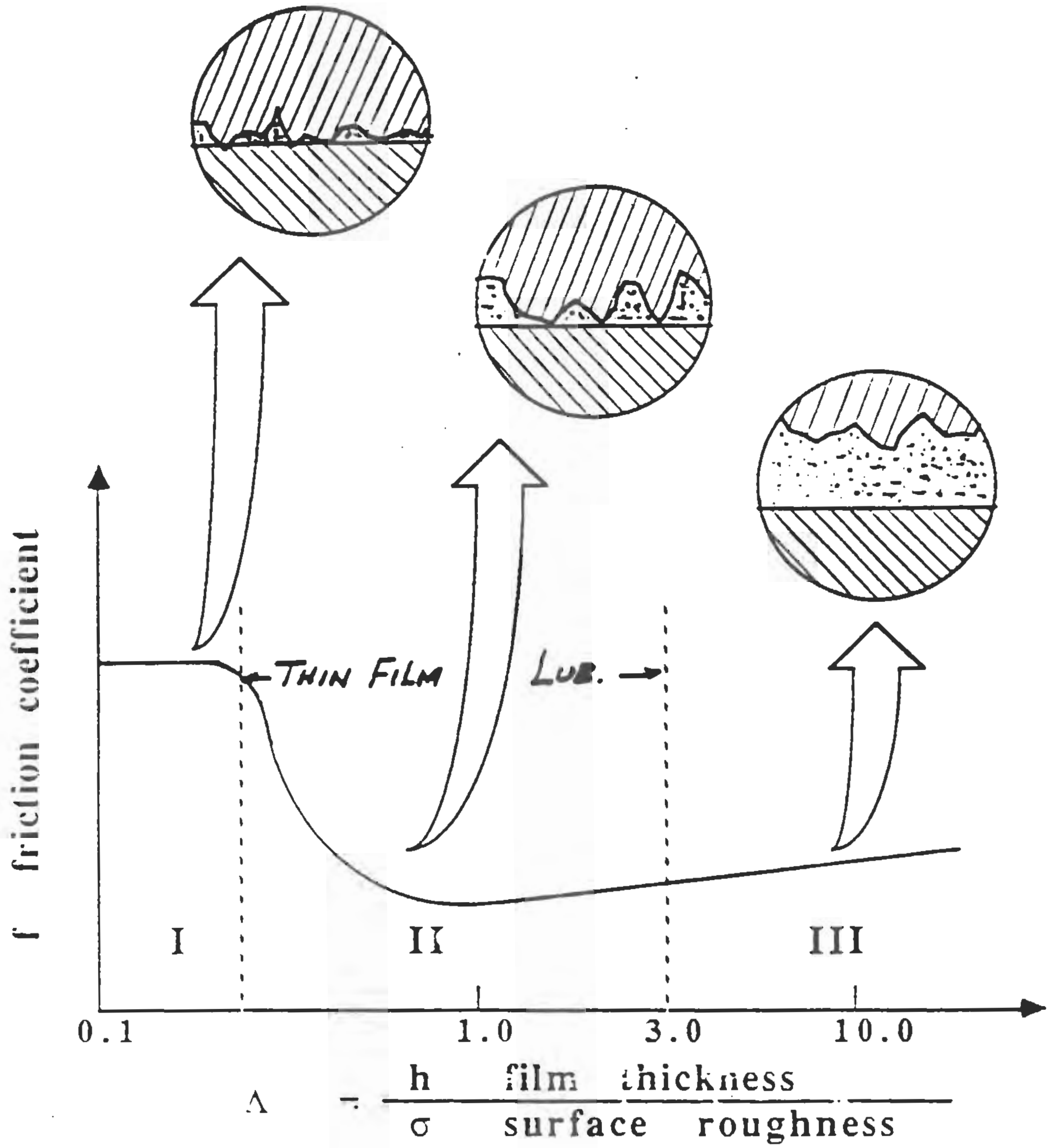

I. Boundary Lubrication

II. Partial E.H.L. (THIN-FILM LUB.)

III. Full Film E.H.L.

Regimes of Lubrication in Lubricated Contacts

Mixed-Film Lubricated Contacts

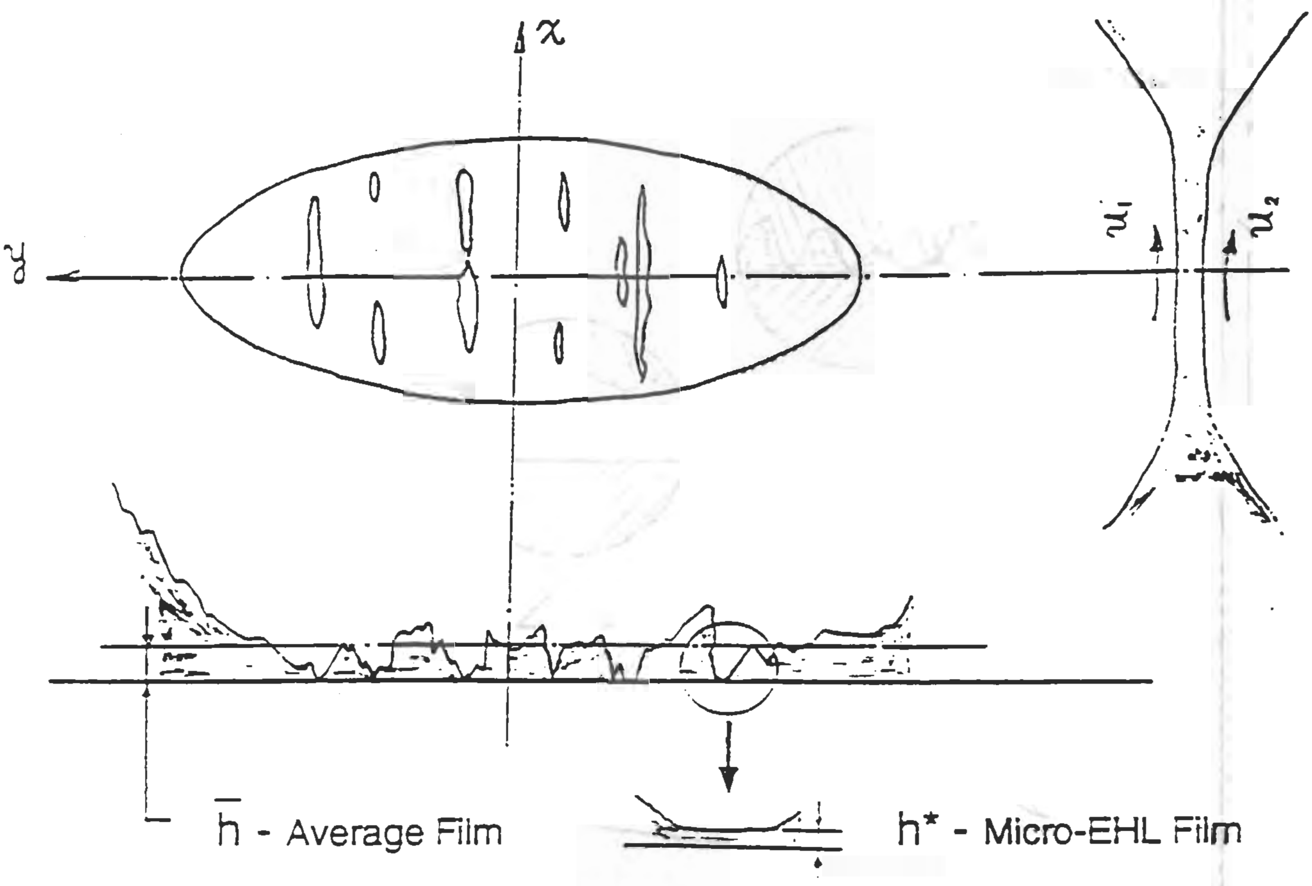

$\bar{h}$ - Average Film

h^* - Micro-EHL Film

$\bar{p}$, $\bar{p}_a$ - Average Fluid and Contact Pressure

p^* - Asperity Contact Pressure

$\bar{\tau}$, $\bar{\tau}_a$ - Average Fluid and Contact Shear Stress

τ^* - Asperity Contact Shear Stress

$\bar{\bar{T}}$, $\bar{T}_a$ - Average Fluid and Contact Surface Temperatures

T^* - Asperity Contact Temperature

CURVE 1 - STANDARD
CURVE 2 - NON-STANDARD

CURVE No.	1	2	
NUMBER OF TEETH (P)	28	28	
NUMBER OF TEETH (G)	33	33	
ADDENDUM OF PINION	5.00	6.50	(MM)
ADDENDUM OF GEAR	5.00	3.50	(MM)
DEDENDUM OF PINION	6.25	4.75	(MM)
DEDENDUM OF GEAR	6.25	7.75	(MM)
PROFILE MODIFICATION	NO	YES	

CURVE No.	1	2	
MODULE	5.0	5.0	(MM)
PRESSURE ANGLE	20.0	25.0	(DEG)
CLEARANCE	1.25	1.25	(MM)
FILLET RADIUS	1.50	1.90	(MM)
TOOTHWIDTH	40.0	40.0	(MM)
ANGULAR SPEED (P)	1450	1450	(RPM)
TORQUE	275	275	(N-M)

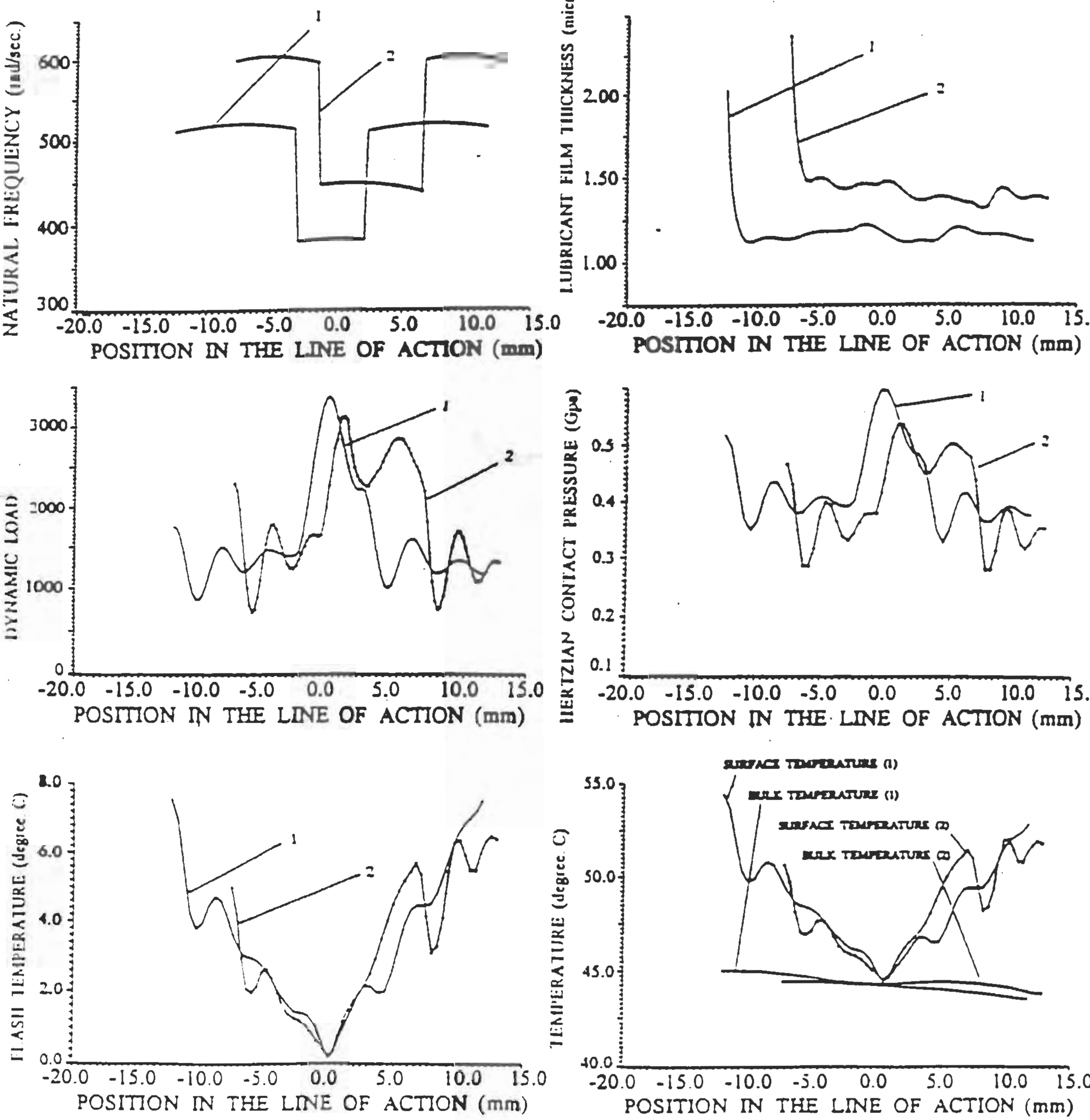

Fig. 12 Comparisons of the Tribological Performances between Standard and Non-Standard Gears

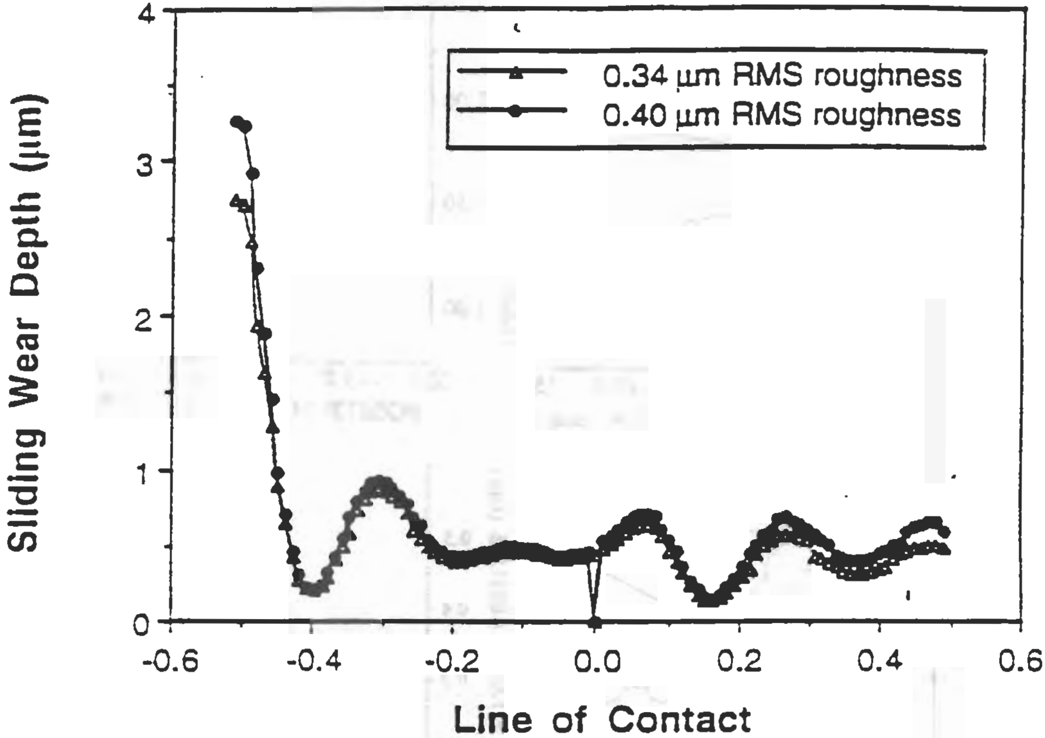

Figure 10. Wear depth distributions of tooth wear profiles after one million cycles

Protective Films and Layers for Sliding Asperities

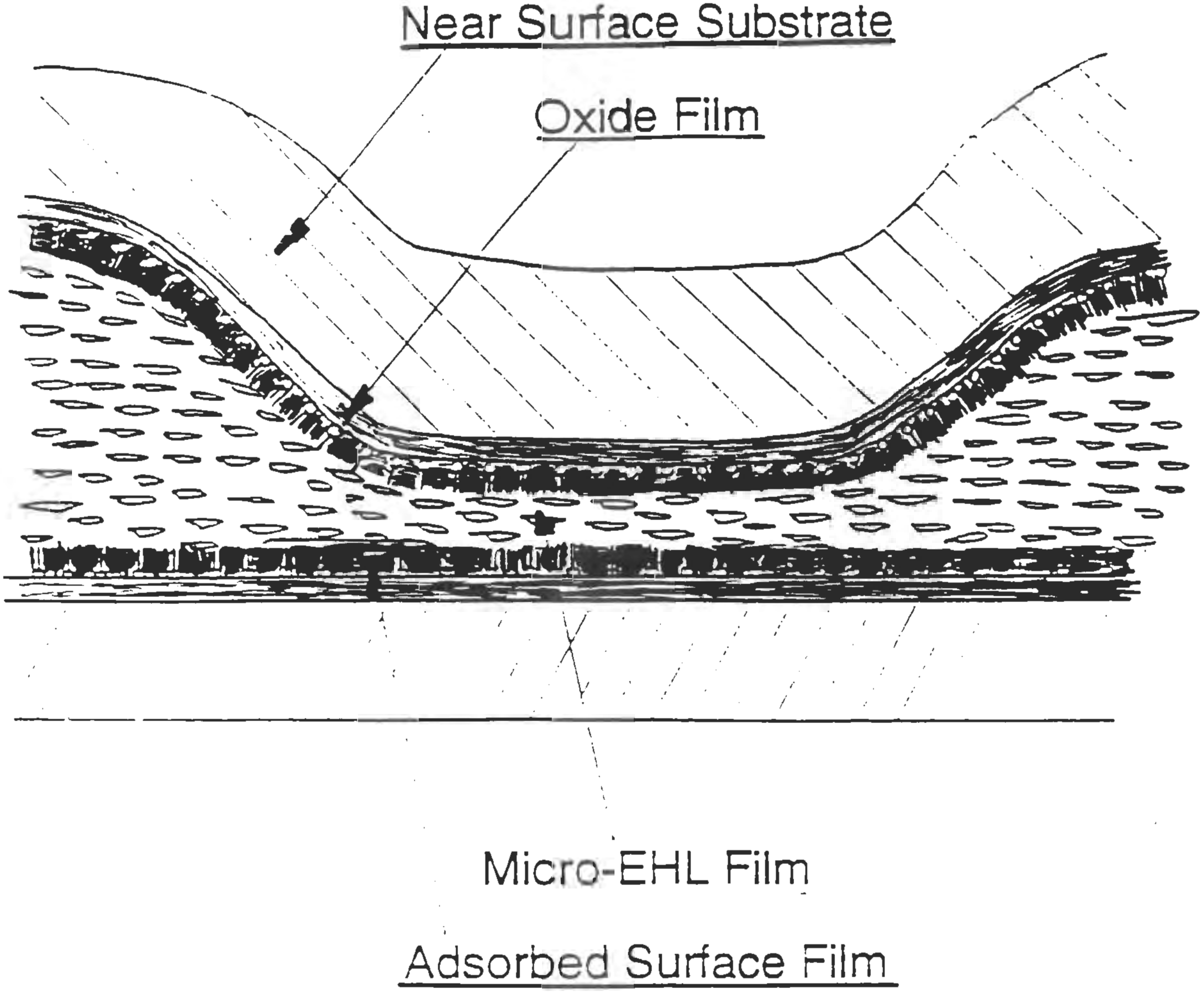

Micro - EHL Film

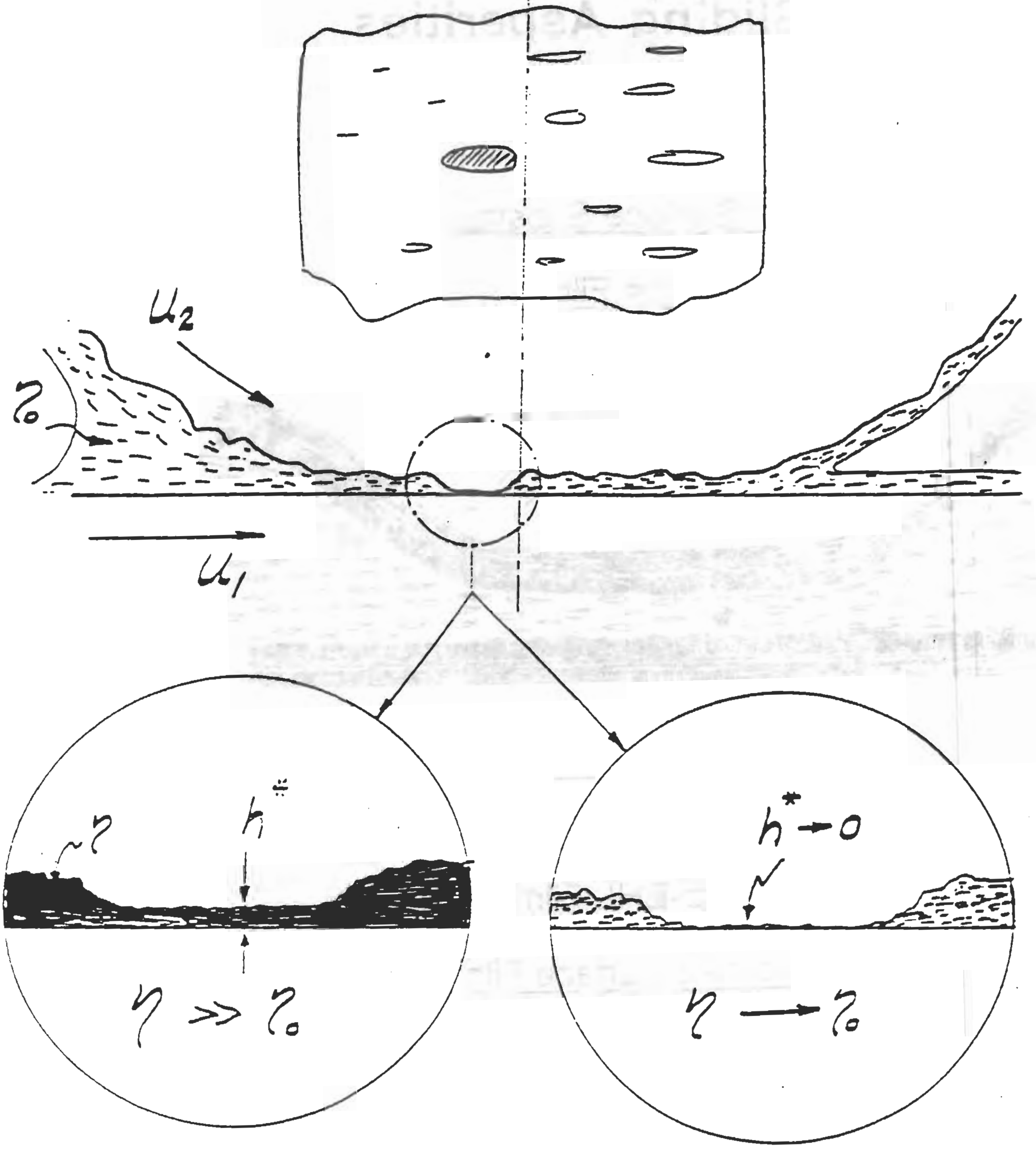

Criterion for Breakdown of Micro - EHL Film

$$Q = 1 - (\eta_o / \eta)$$

$$= 1 - e^{-\alpha p}$$

$\eta >> \eta_o$; $Q \rightarrow 1$ Micro-EHL Effective

$\eta \rightarrow \eta_o$; $Q < 1$ Micro- EHL Breakdown

SCUFFING EXPERIMENT RESULTS CORRELATED WITH DYSON'S Q-MECHANISM THEORY. THIS IS FOR TEST CASES WHICH UNDERWENT MACROSCOPIC SCUFFING FAILURE. THE LUBRICANT USED WAS STRAIGHT MINERAL OIL.

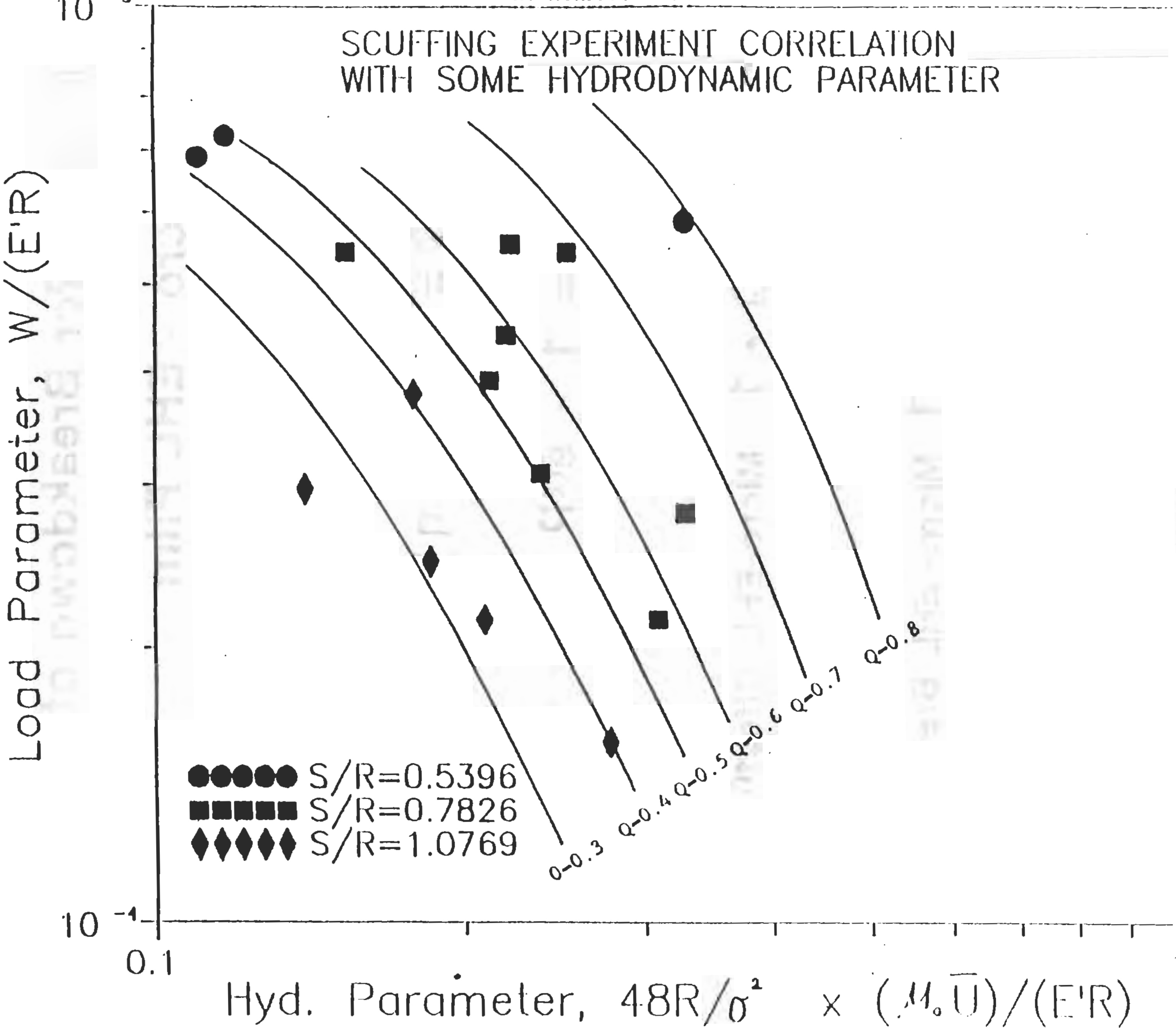

ADSORPED SURFACE FILM

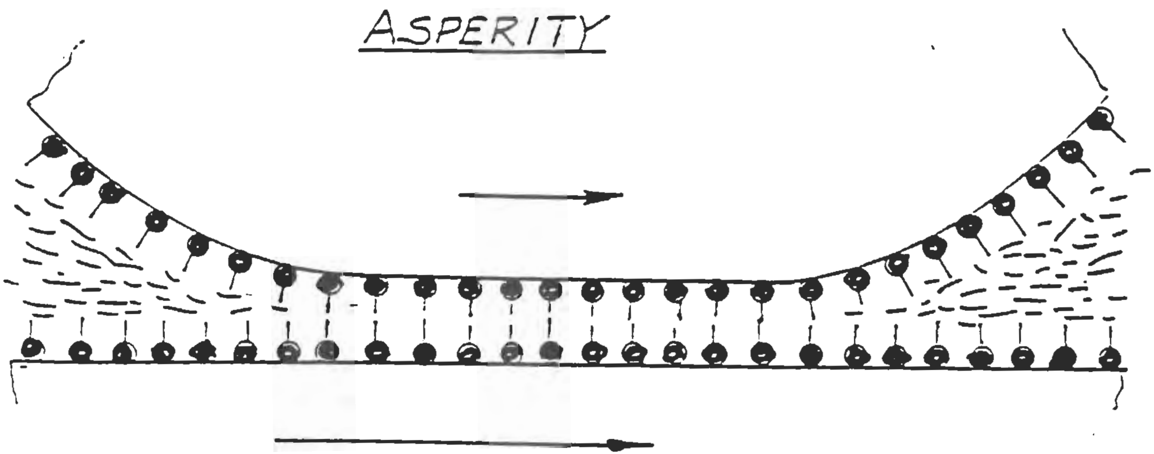

ASSUMPTIONS ON LANGMUIR'S EQUATION

) Adsorption is terminated at one monolayer of the adsorbate.

2) The molecules are non-interacting but only competes for a fixed number of sites all having the same activation energy Ea.

3) The vibrational and rotational excitations of the molecules are negligible.

4) The lubricant and the surface is in thermal equilibrium.

5) The molecular kinetics for the lubricant are governed by the ideal gas law.

Thus applying Langmuir's adsorption isotherm theory, the fractional coverage of the adsorbate is given by:

$$\theta = \frac{F}{F + \frac{K_b T}{\hbar} \frac{2\pi m K_b T}{\hbar^2} \exp\left(\frac{-\Delta H_{ads}}{K_b T}\right)}$$

where $$F = \frac{P}{\sqrt{2\pi m K_b T}}$$

this term represents the molecular bombardment rate of the lubricant molecules on to the surface.

MODELING

OF

ADSORBED SURFACE FILM

ADSORPTION AS A FUNCTION OF PRESSURE AND TEMPERATURE

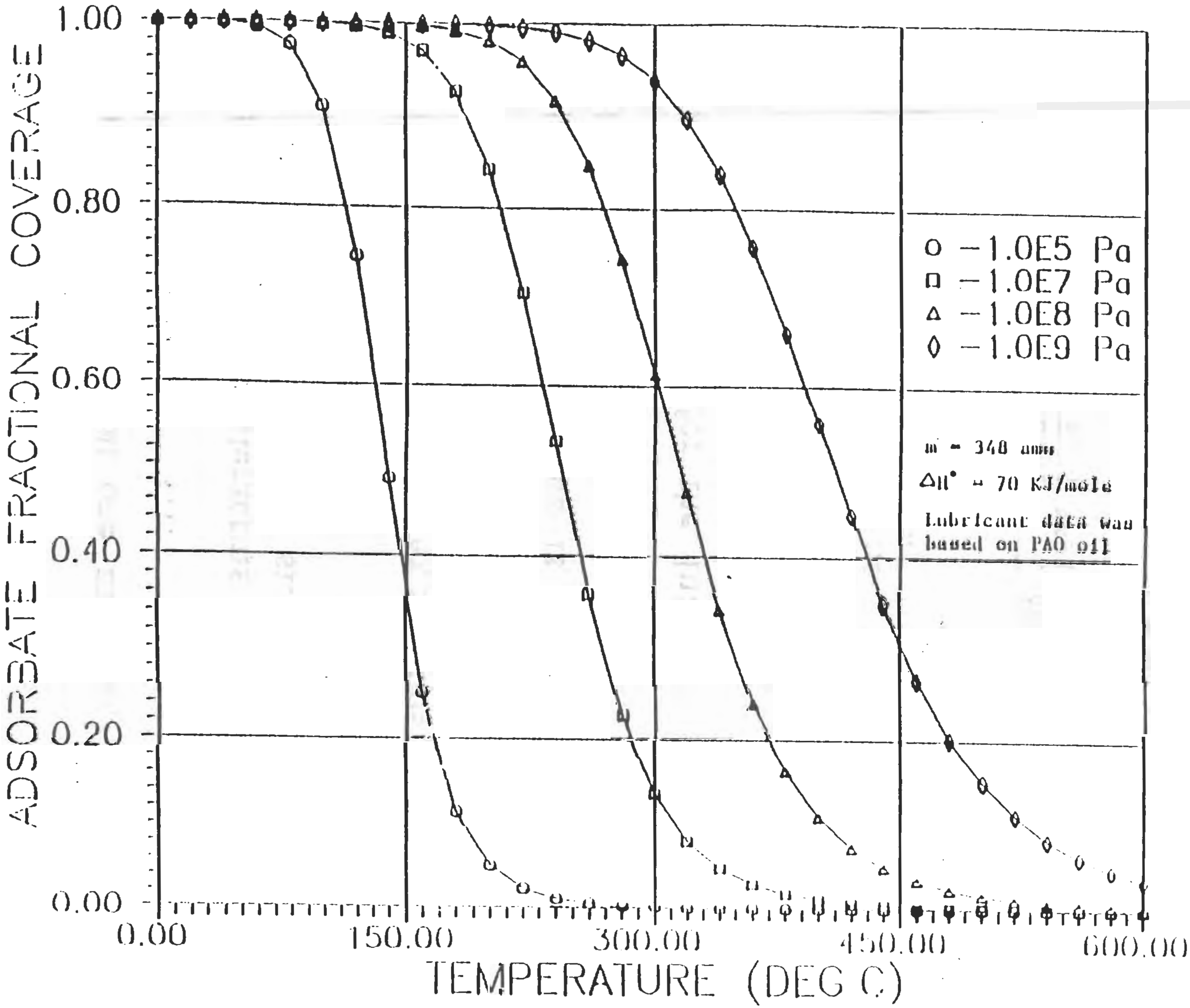

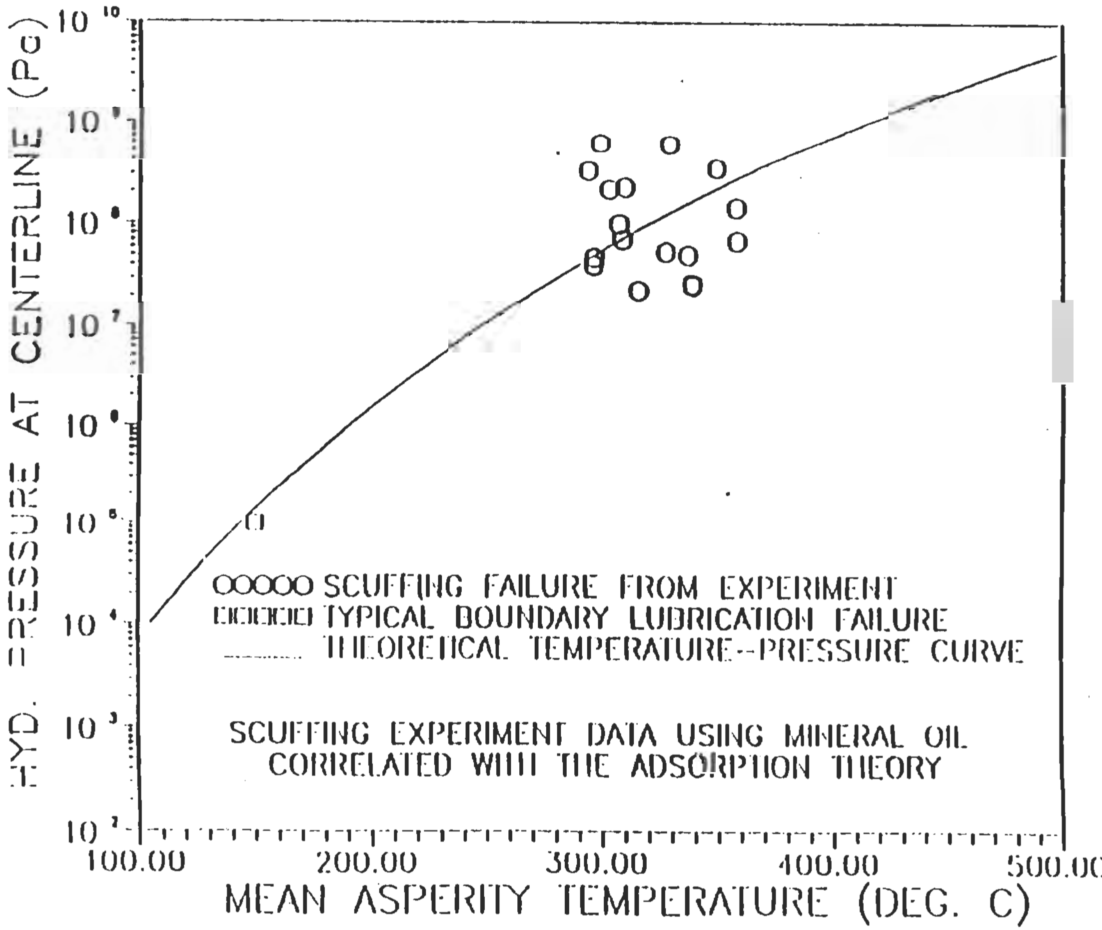
HYD. PRESSURE AT CENTERLINE (Pa)
10 10
10 9
10 8
10 7
10 6
10 5
10 4
10 3
10 2
100.00
200.00
300.00
400.00
500.00
MEAN ASPERITY TEMPERATURE (DEG. C)
OOOOO SCUFFING FAILURE FROM EXPERIMENT
TYPICAL BOUNDARY LUBRICATION FAILURE
THEORETICAL TEMPERATURE--PRESSURE CURVE
SCUFFING EXPERIMENT DATA USING MINERAL OIL
CORRELATED WITH THE ADSORPTION THEORY

Figure 46

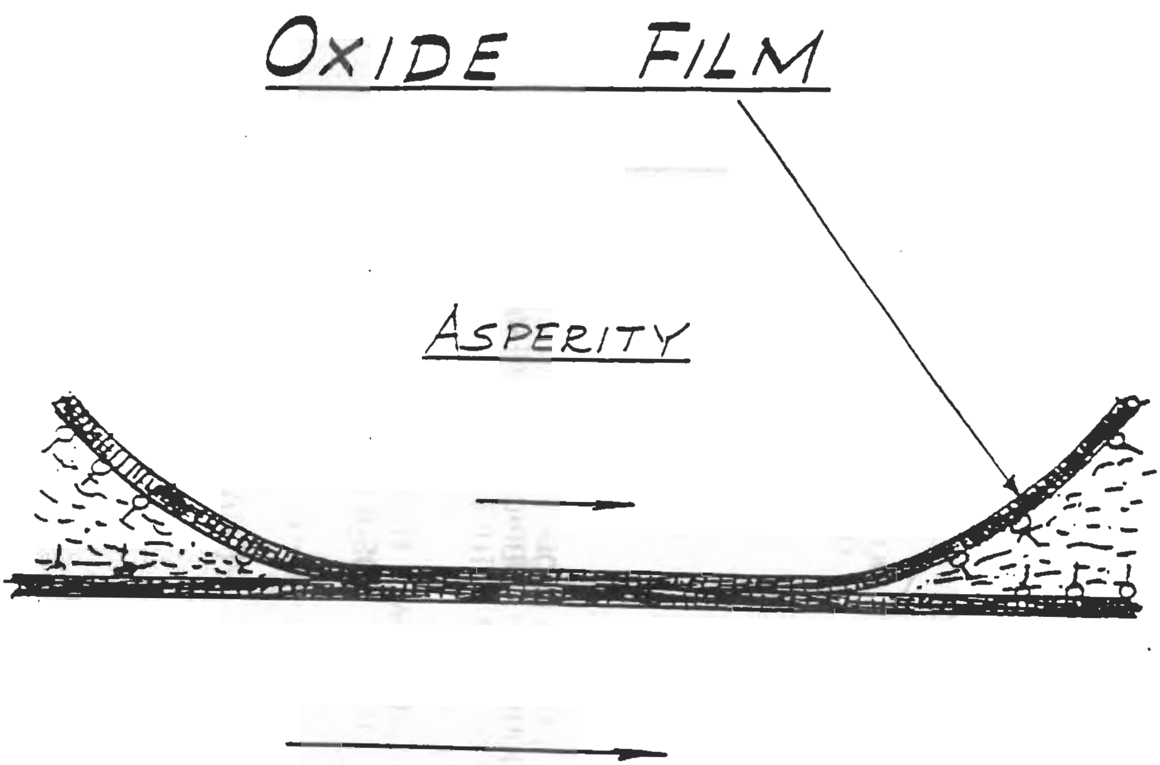

Metal oxide thickness increase:

$$\xi_m = C A_r e^{\frac{-Q}{RT}} t$$

C is a constant dependent upon the metal oxide composition

Metal oxide thickness decrease by Wear:

$$k = k_m \frac{X}{U t_o} e^{\frac{-E}{RT}}$$ from C. Rowe's works

$$\xi_w = k_m \frac{X}{t_o} e^{\frac{-E}{RT}} \frac{Lt}{HA}$$

L = load
H = hardness
A = area

Metal oxidation process:

$$\Delta m = A_r e^{\frac{-Q}{RT}} . t$$

A_r = Arrhenius constant
Q = oxidation activation energy

A_r, Q used in the present work are

$A_r = 7.278 \times 10^{-4}\ g/cm^2$ - sec
Q = 26 KJ/mole

Metal oxide thickness increase:

$$\xi_m = CA_r e^{\frac{-Q}{RT}} . t$$

C is a constant dependent upon the metal oxide composition

Metal oxide thickness decrease by Wear:

$$k = k_m \frac{X}{Ut_o} e^{\frac{-E}{RT}}$$ from C. Rowe's works

$$\xi_w = k_m \frac{X}{t_o} e^{\frac{-E}{RT}} \frac{Lt}{HA}$$

L = load
H = hardness
A = area

Criterion for scuffing failure to occure:

$$\Delta\xi = \xi_m - \xi_w$$

For different operating conditions, when the formation of metal oxide is no longer faster than the removal process by wear, scuffing will occur eventually.

According to the previously mentioned processes, the oxygen content in the lubricant may be totally depleted, which controlls the formation and removal of the metal oxide.

Oxidation Test

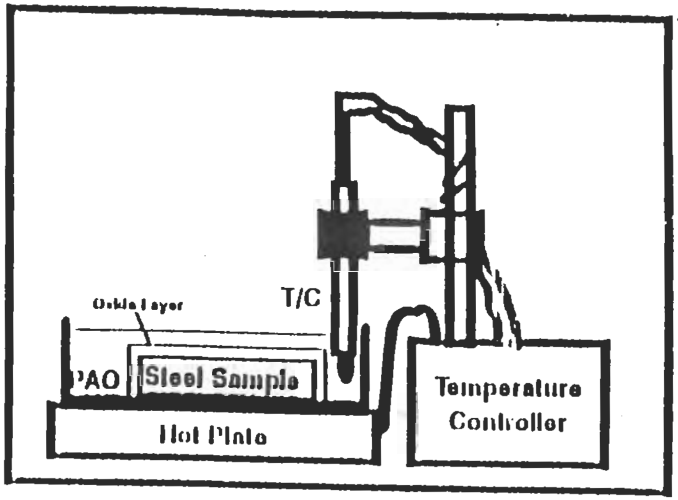

Oxide Removal in Vacuum

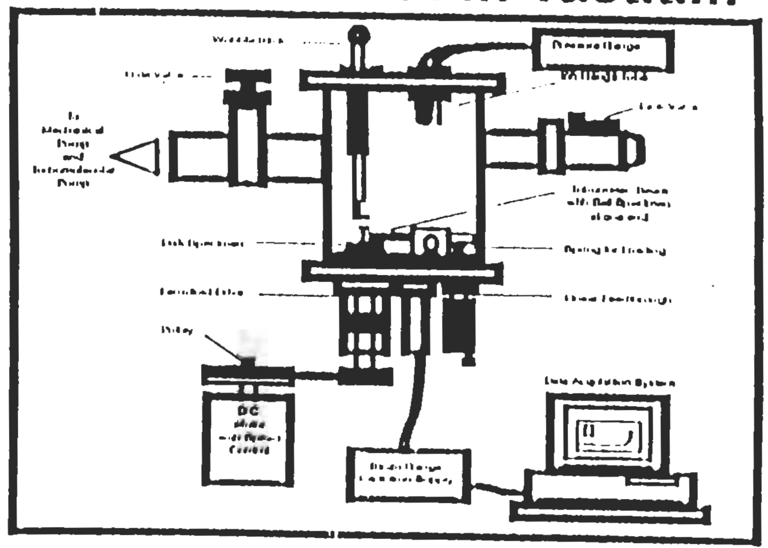

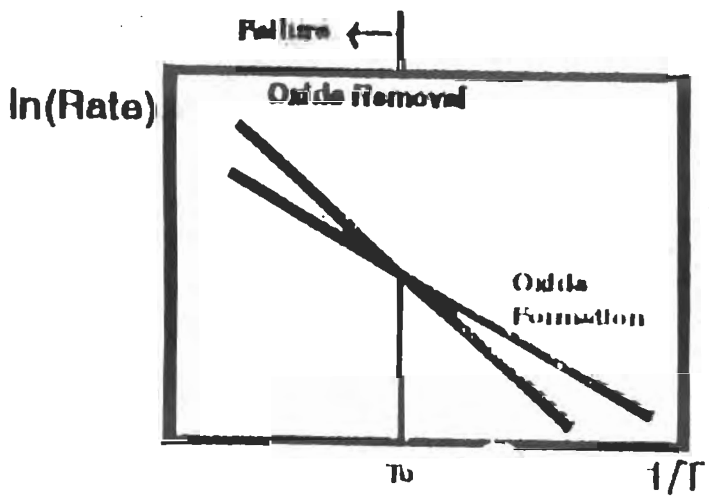

Oxide Formation:

$$R_f = \nu_f e^{-E_f/RT}$$

Oxide Removal:

$$R_r = \nu_r e^{-E_r/RT}$$

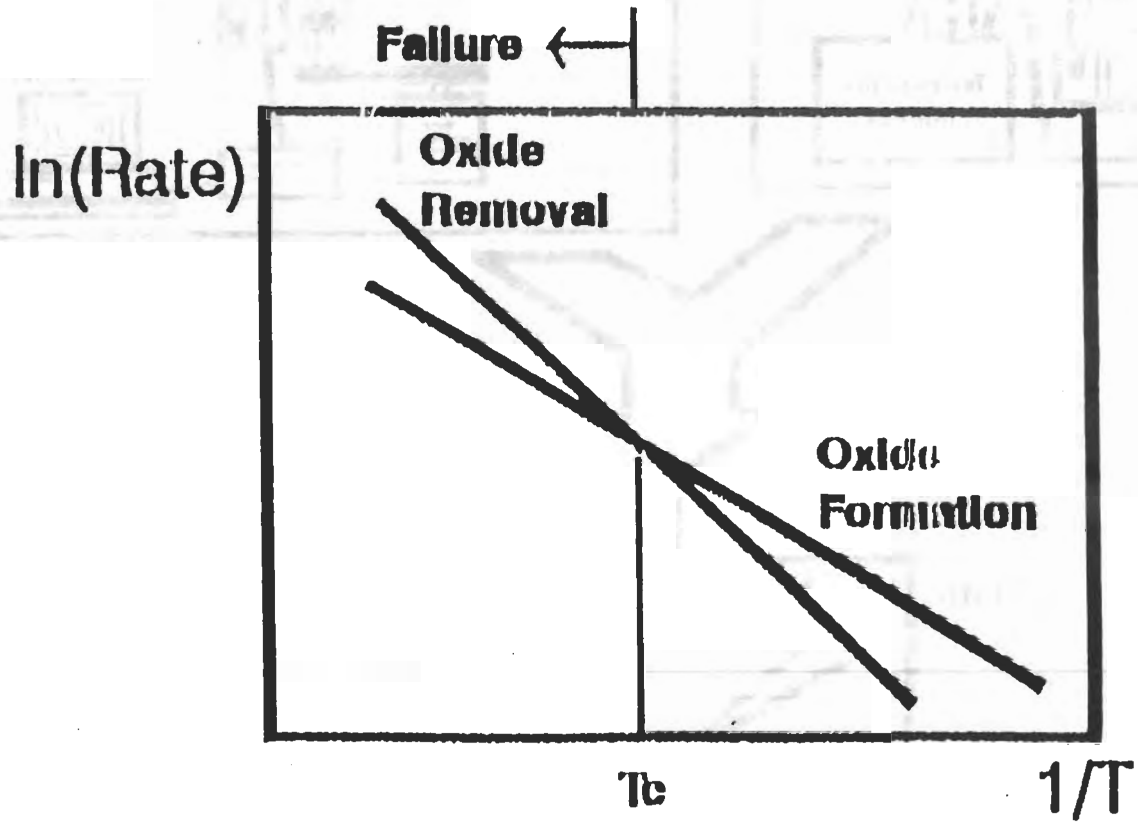

Failure of Substrate

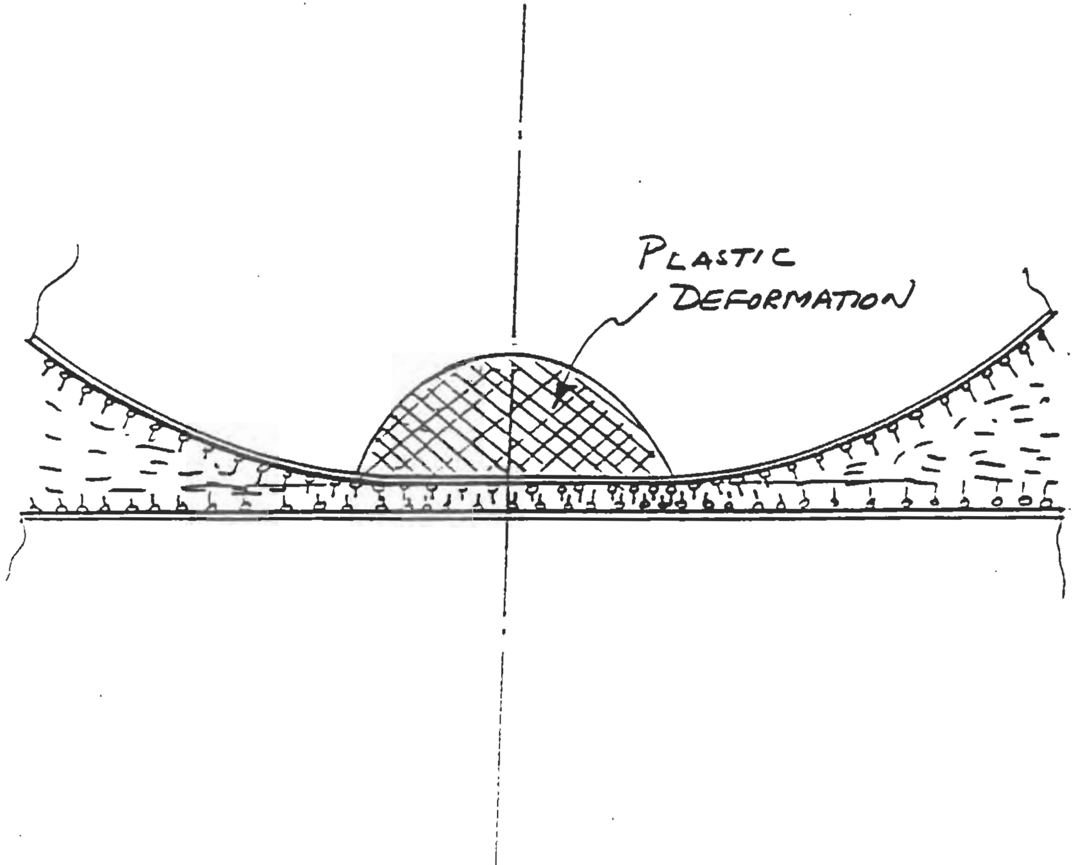

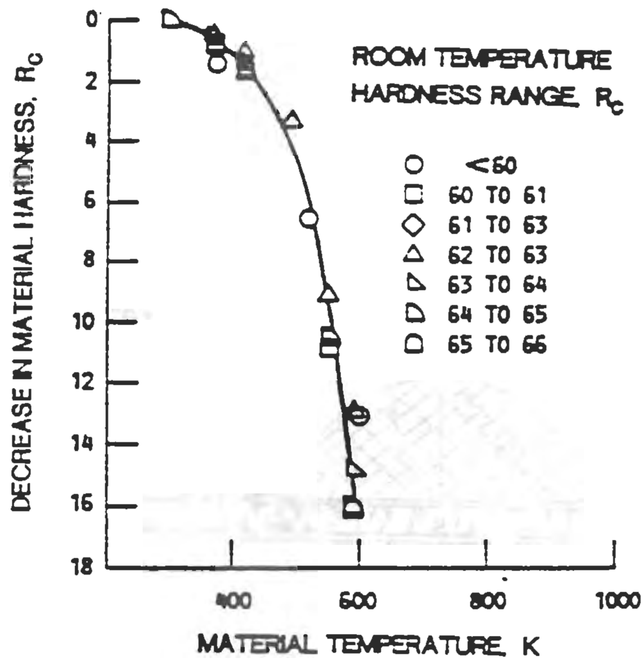

Fig. 7 Hardness of AISI 52100 as a function of Temperature. (From Zaretsky, 1988.)

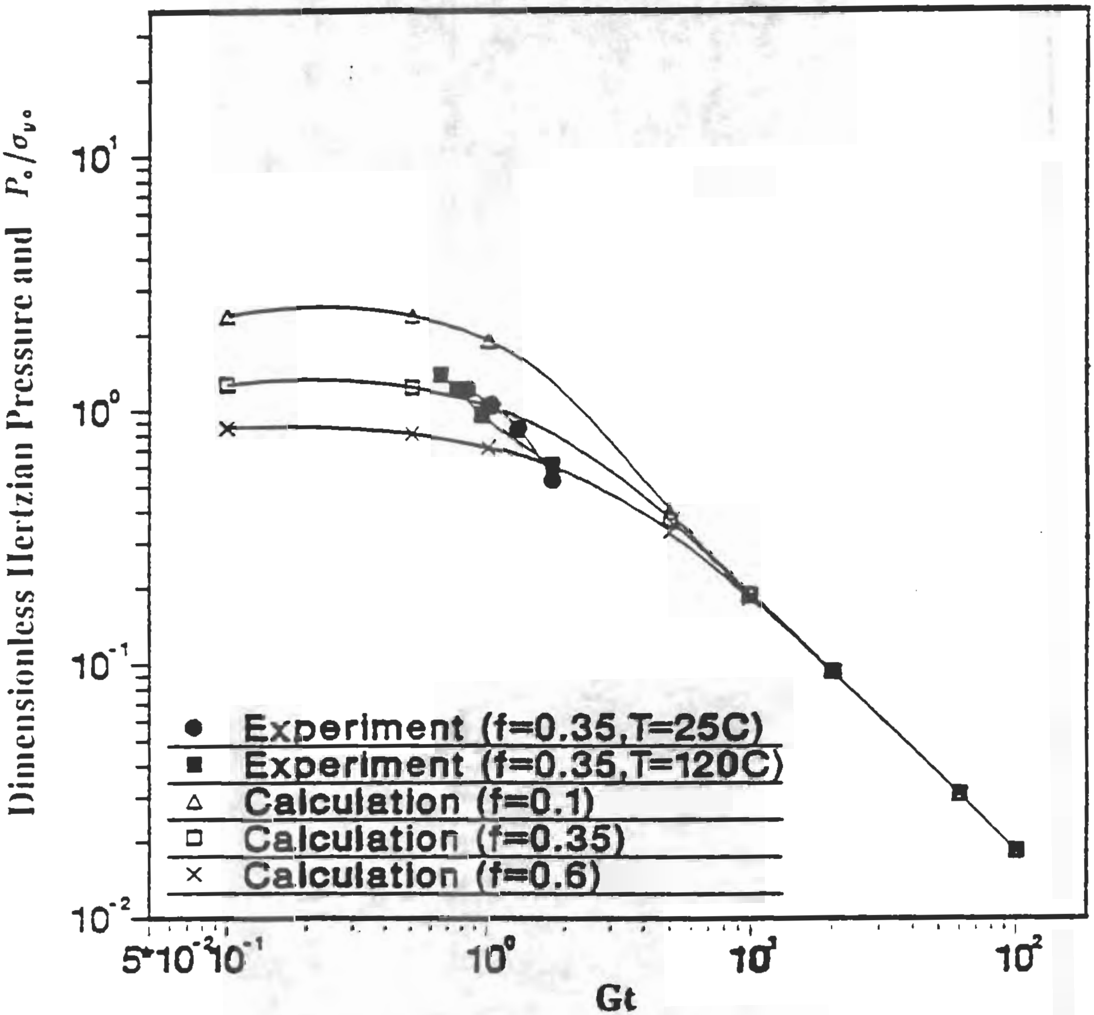

Fig. 9 Comparison between the Calculation and Experimental Data for AISI 52100 in SAE 10W base oil (Fo=0.1; T=25C and T=120C)

POSTULATED SCUFFING MECHANISM

- Lubrication Breakdowns Leading to Microscuffing

- Transition from Micro to Macroscuffing

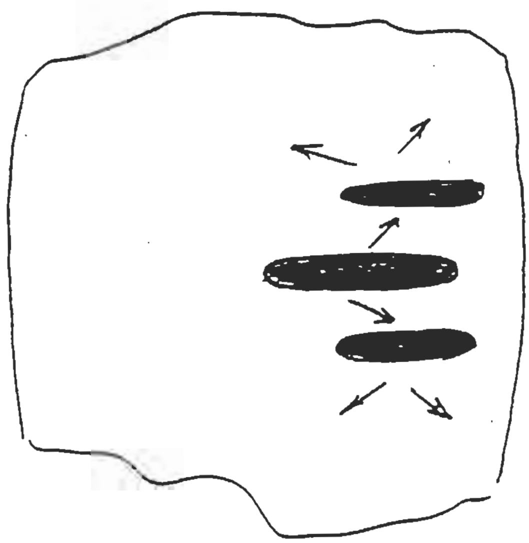

Scuffing Test

Experimental Setup

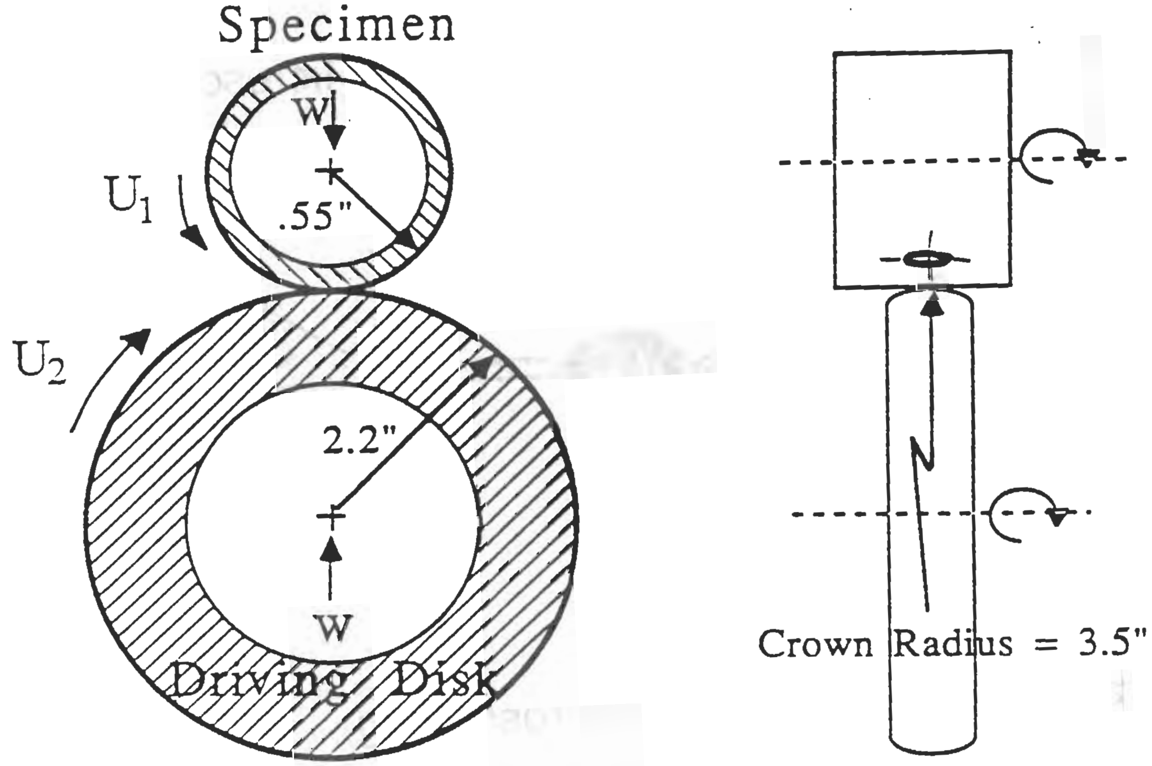

(Specimen Setup) (Side View)

Loading Stage

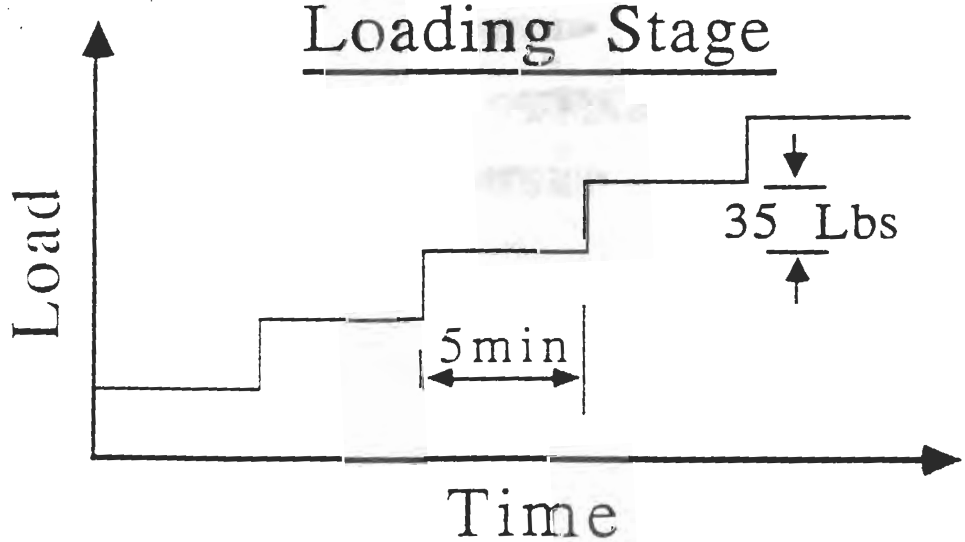

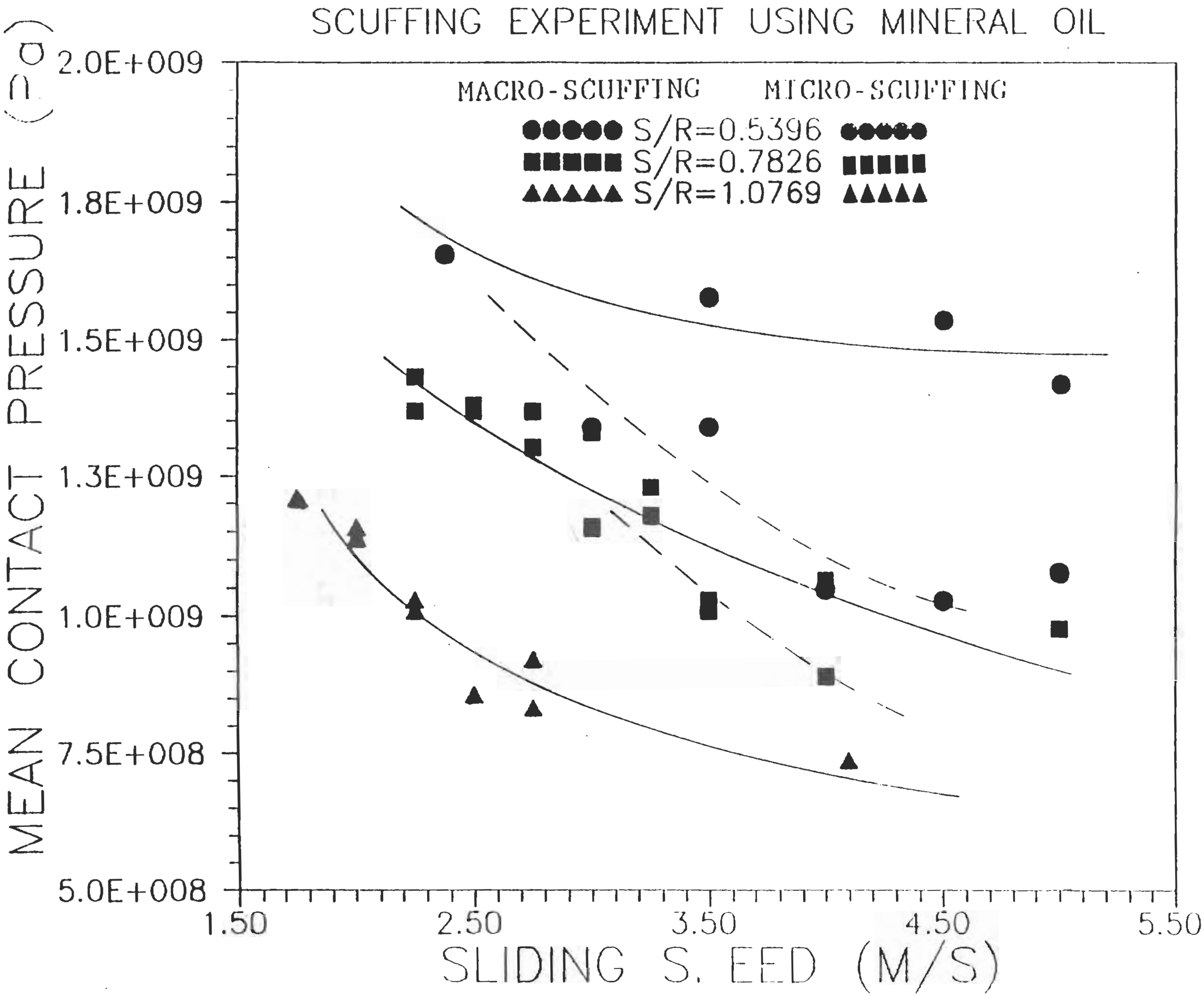
SCUFFING EXPERIMENT USING MINERAL OIL
MEAN CONTACT PRESSURE (Pa)
SLIDING S. EED (M/S)
MACRO-SCUFFING
MICRO-SCUFFING
S/R=0.5396
S/R=0.7826
S/R=1.0769
2.0E+009
1.8E+009
1.5E+009
1.3E+009
1.0E+009
7.5E+008
5.0E+008
1.50
2.50
3.50
4.50
5.50

CONCLUDING REMARKS

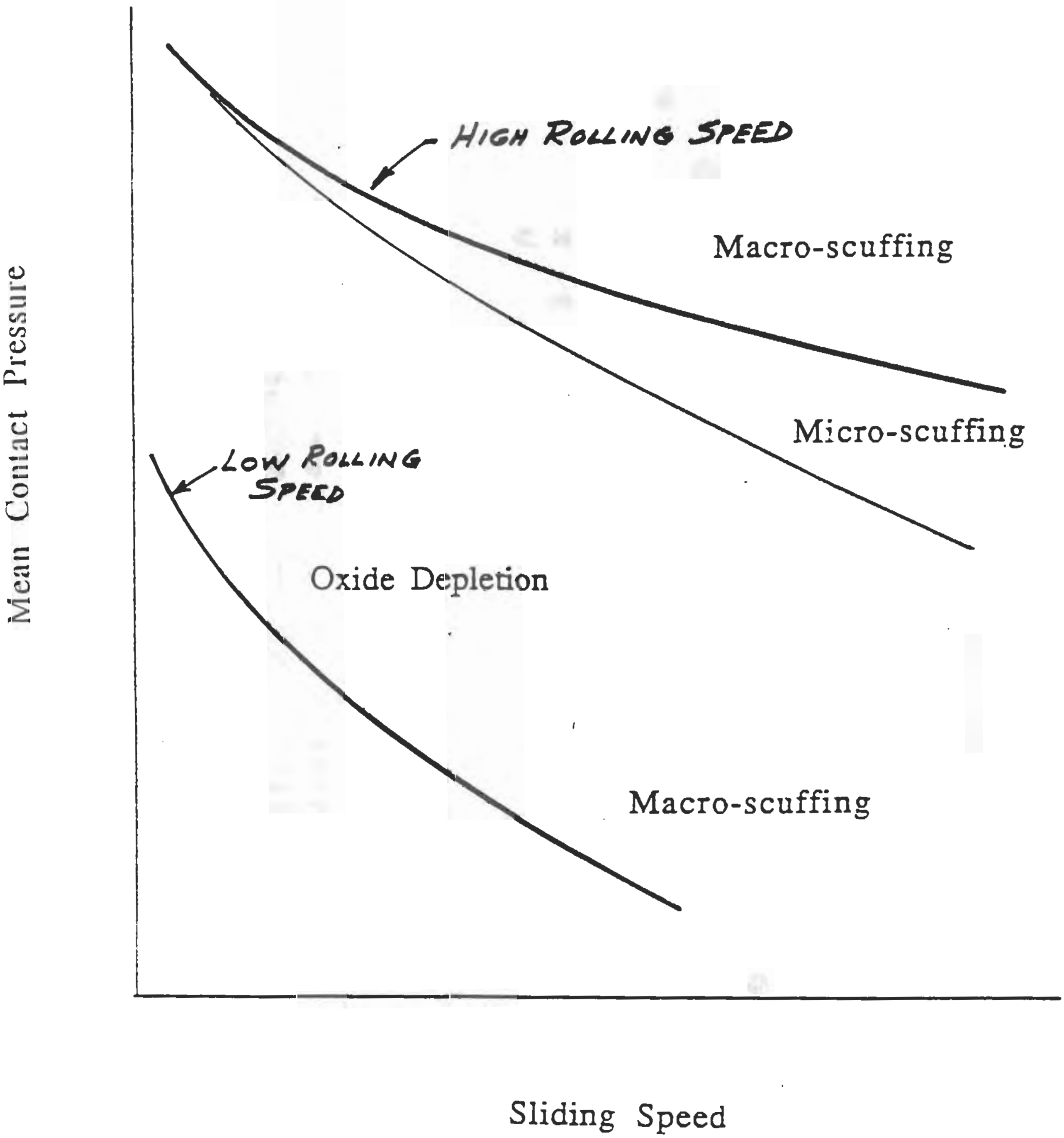

Postulated Successive Modes of Sliding Failure

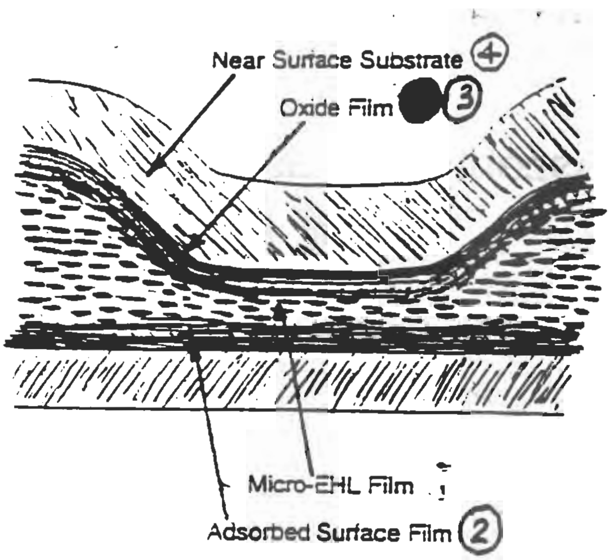

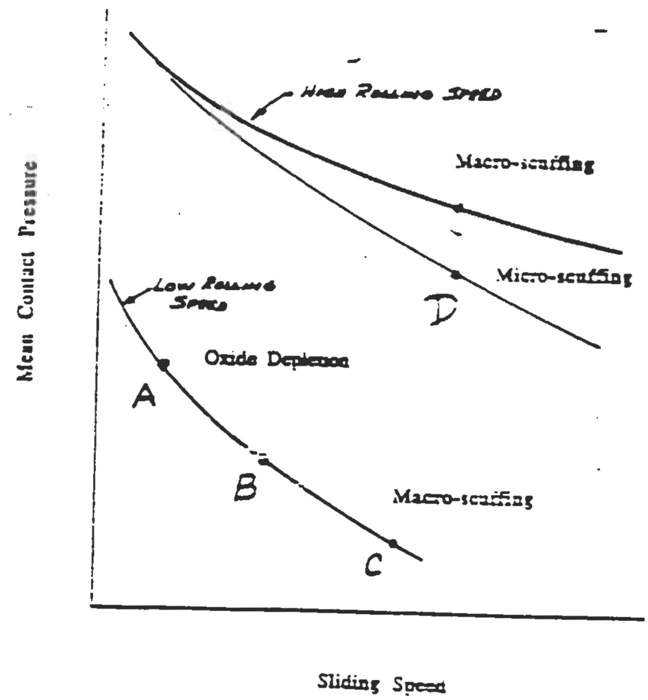

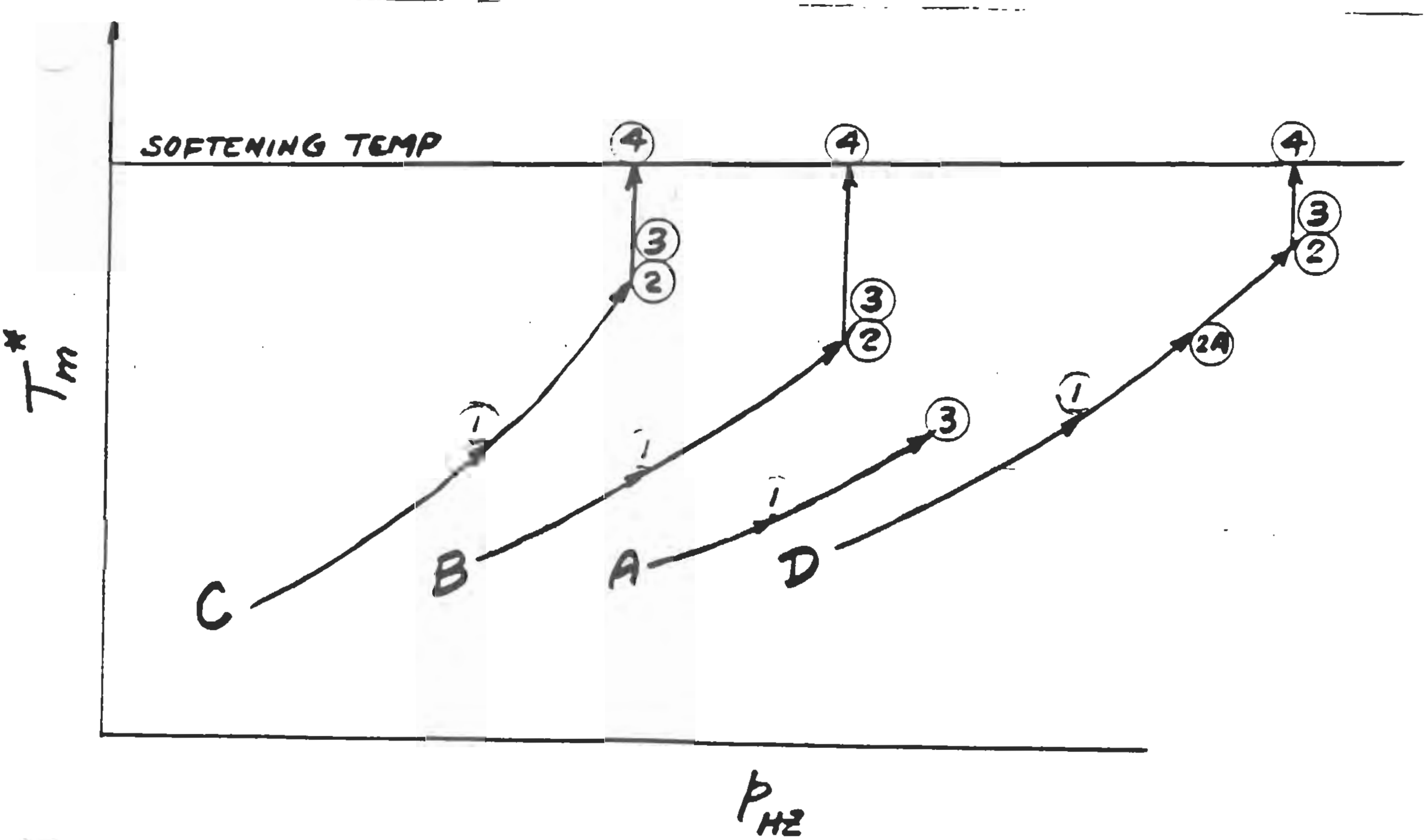

Postulated Mechanism for Surface Pitting

- Crack Initiation from Asperity Contact

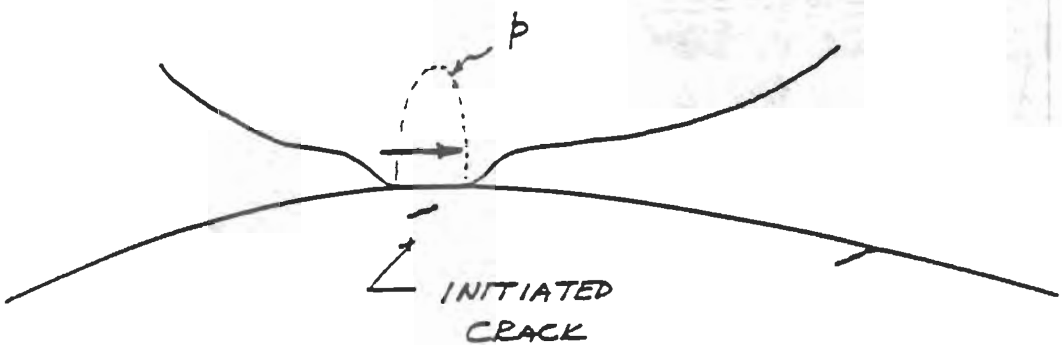

- Crack Propagation to Pitting

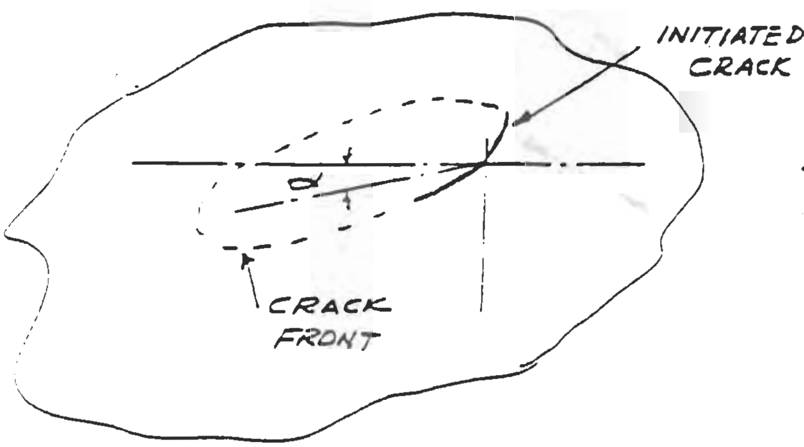

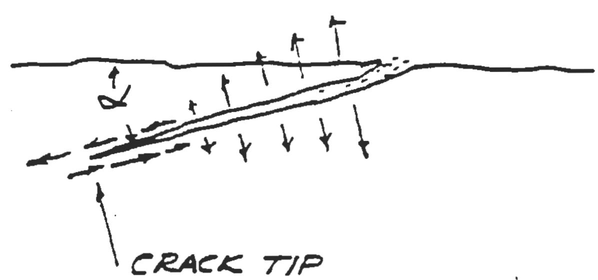

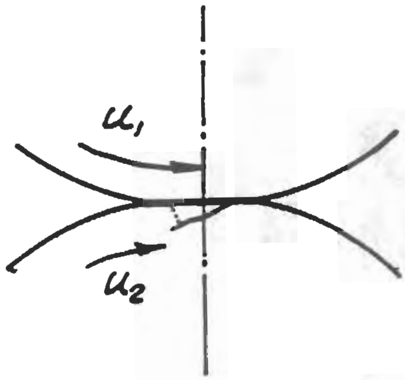

u_1
u_2

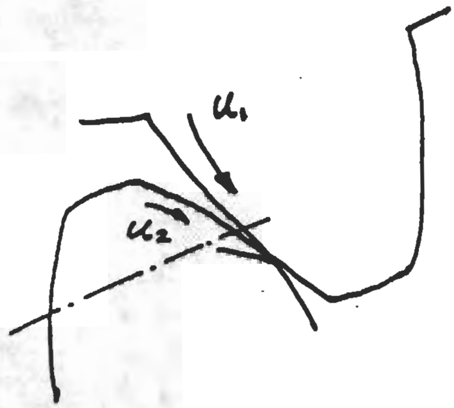

u_1
u_2

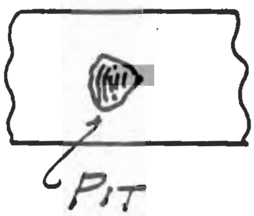

PIT

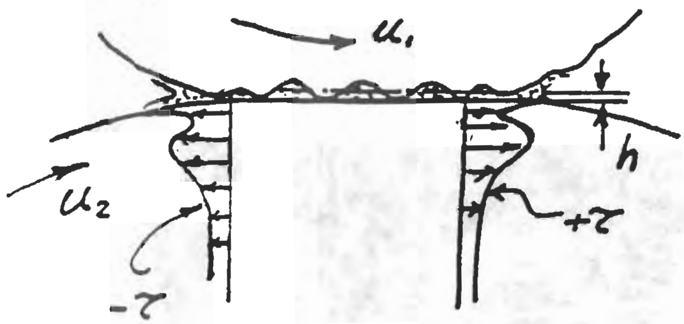

u_1
u_2
h
$+\tau$
$-\tau$

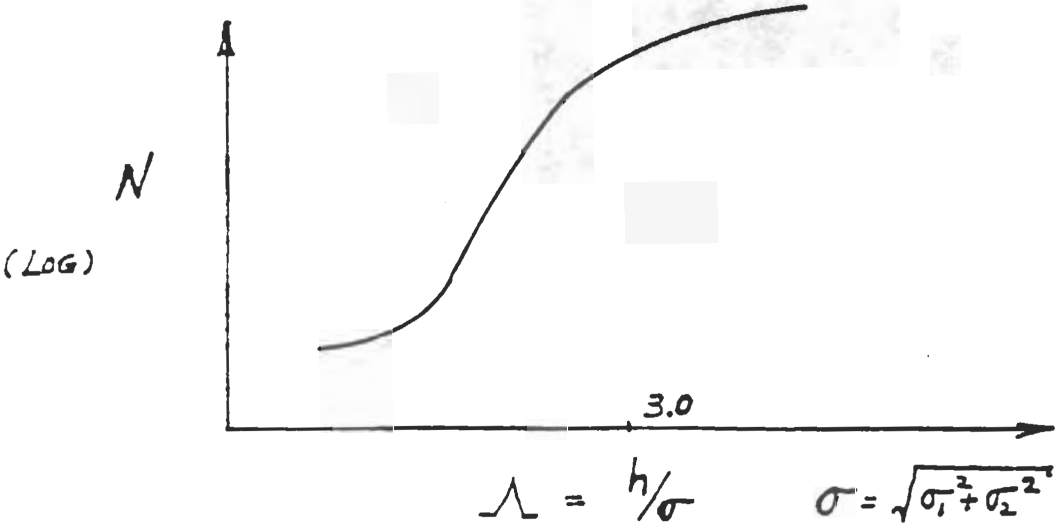

N
(LOG)
3.0
$\Lambda = h/\sigma$
$\sigma = \sqrt{\sigma_1^2 + \sigma_2^2}$

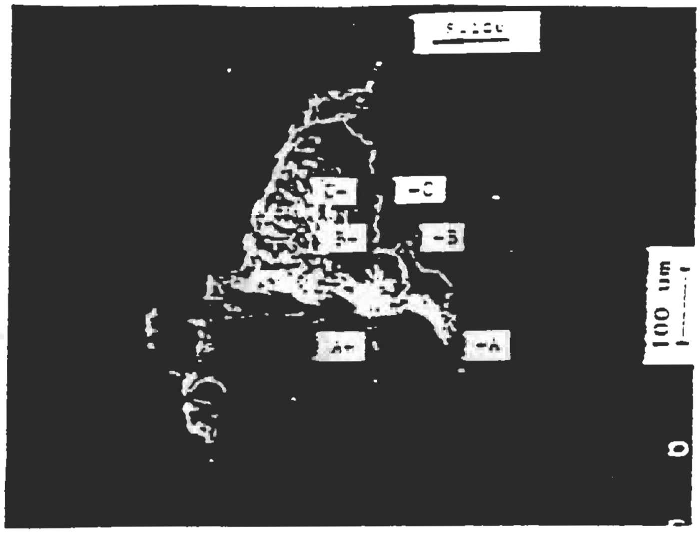

Fig. 3.12 (a) A pit on the surface of 52100 specimen after 4.5 million cycles at 335 KSI maximum Hertzian contact pressure and 0.25 slide-to-roll ratio

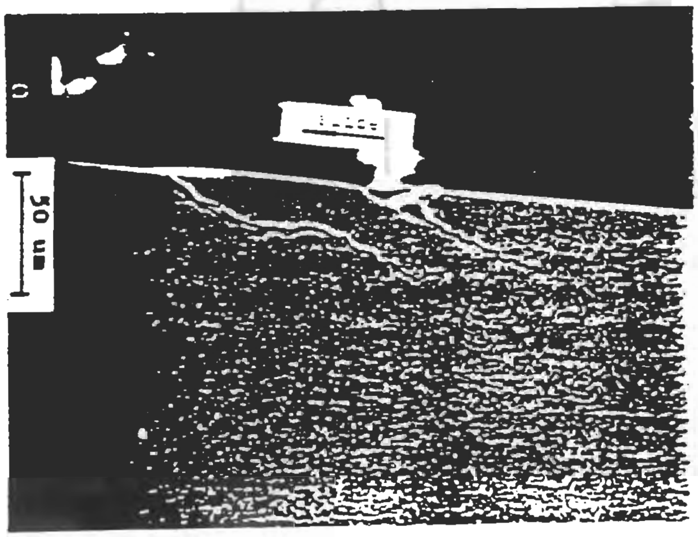

Fig. 3.12 (b) A-A section of the pit in Fig. 3.12 (a).

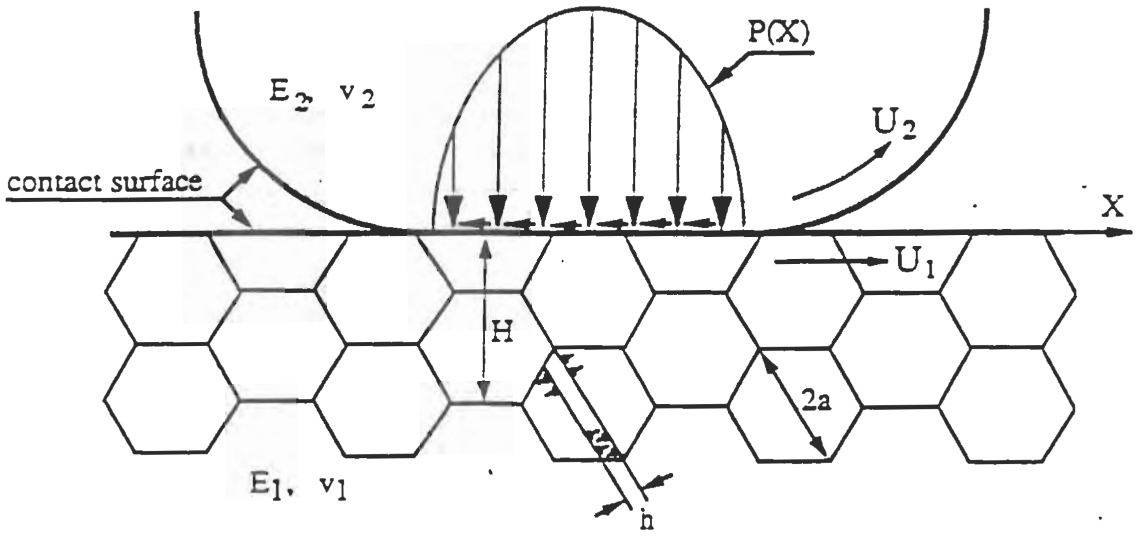

2a = grain or subgrain size
h = width of slip band.
B = half-width of Hertzian contact zone
H = depth of crack initiation from contact surface

Three cases:

(i) $0 \le H < 2\ \mu m$, surface crack initiation;
(ii) $2\ \mu m < H < 0.4B$, near surface crack initiation;
(iii) $0.4B < H$, substrate crack initiation.

Fig. 1. Modeling of crack initiation under contact fatigue.

Surface Crack Initiation Life, ni

Fig. 8. Model prediction of effect of hardness on crack initiation life (q=3.8).

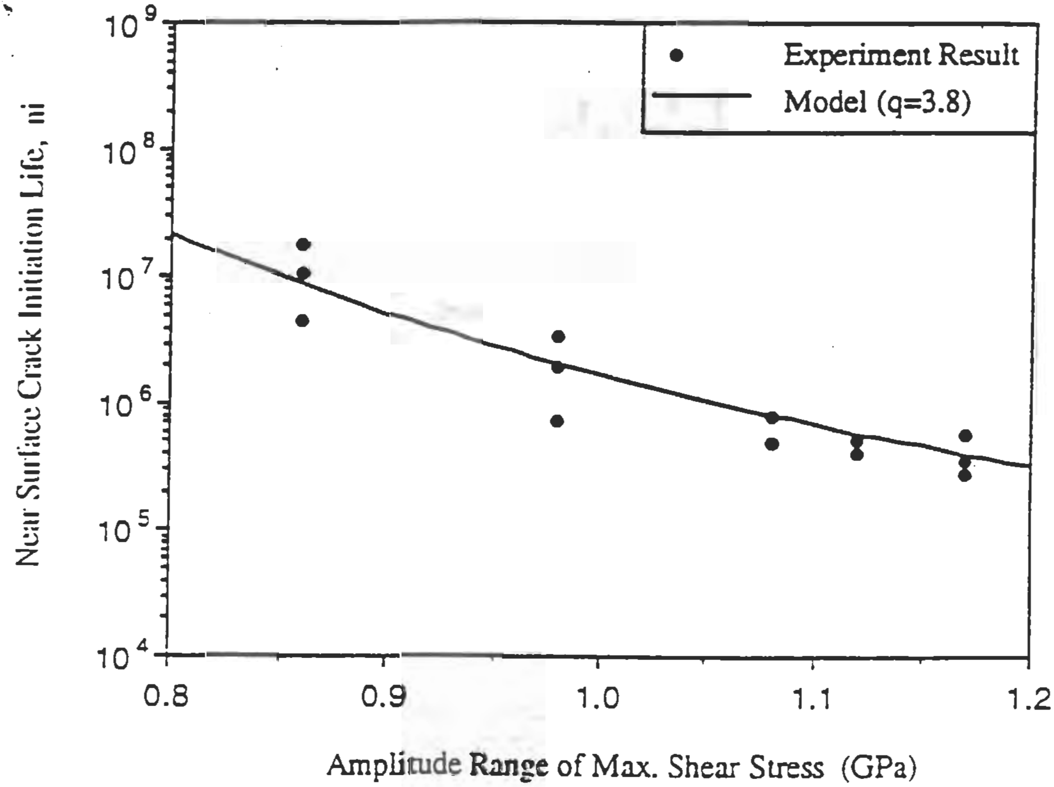

Fig. 7. Comparison of model prediction with experimental results (Zhou, et al. 1989) about near surface crack initiation life (Rc = 62.5).

PROBLEM CONFIGURATION FOR CONTACT FATIGUE

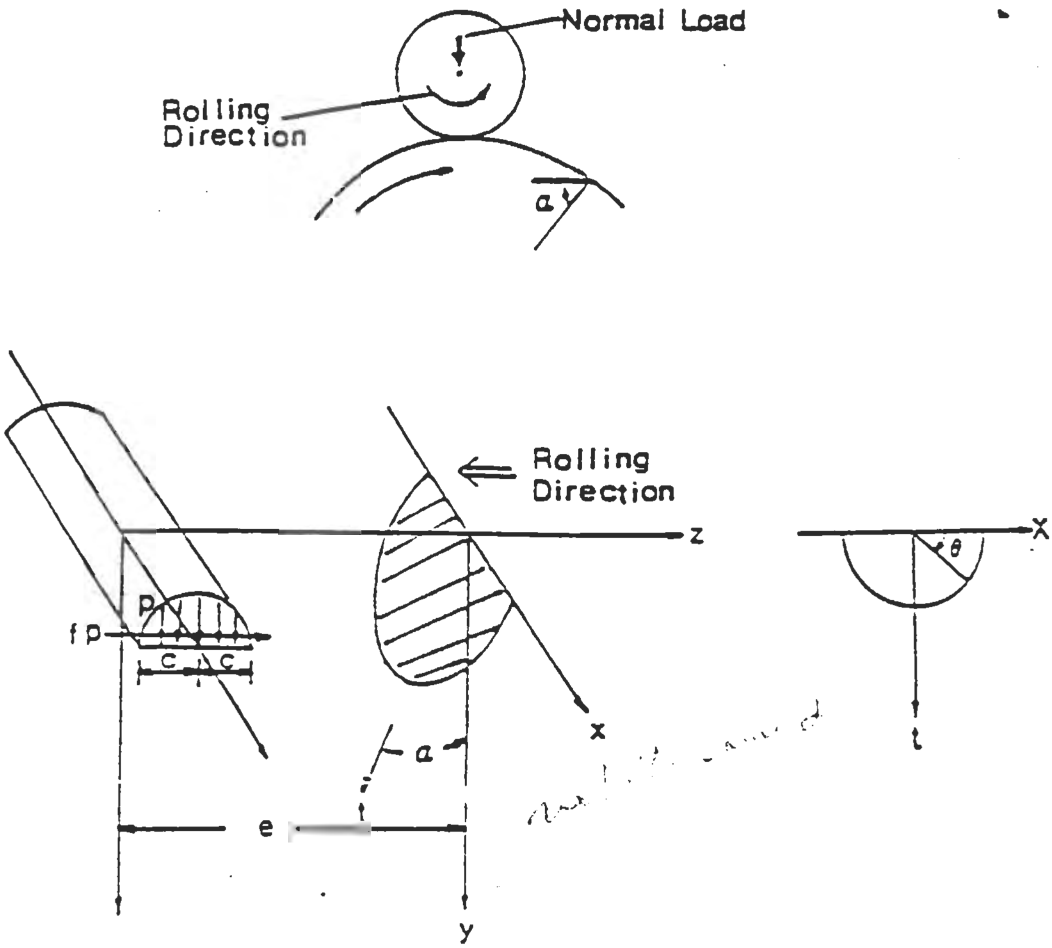

Figure 3. Geometry and coordinate system for crack propagation model.

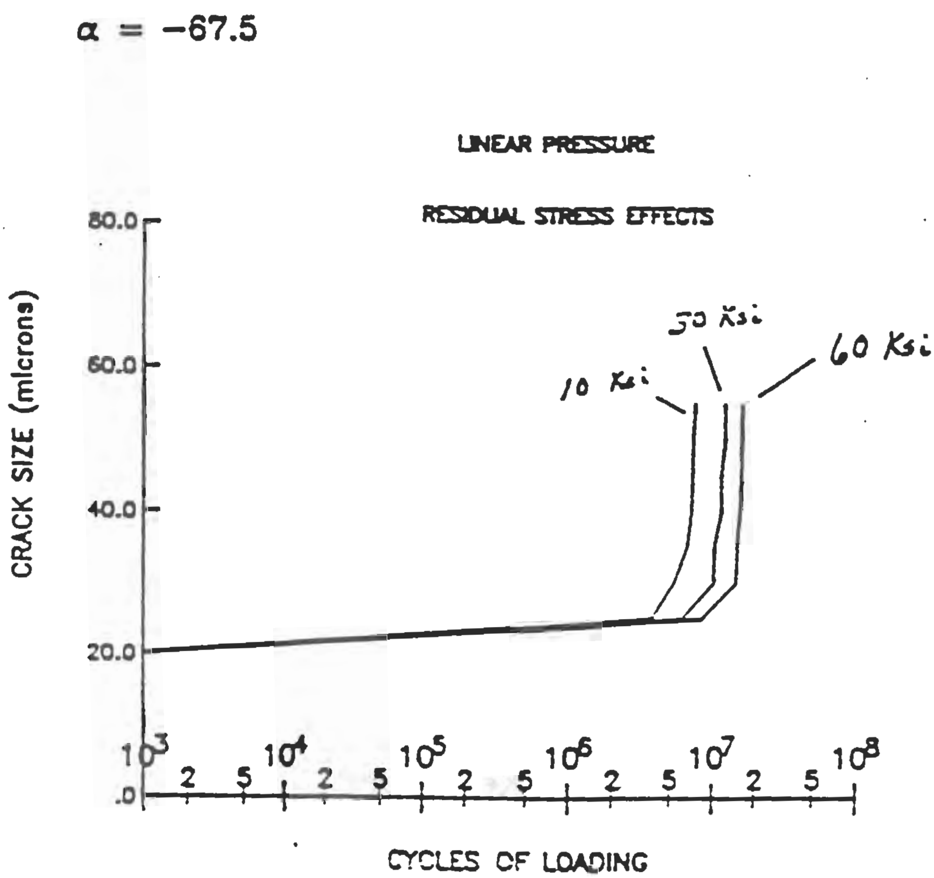

Figure 11 Predicted crack size versus loading cycles for a crack inclined at 22.5 degrees from the surface under linear fluid pressure including residual stress effects.

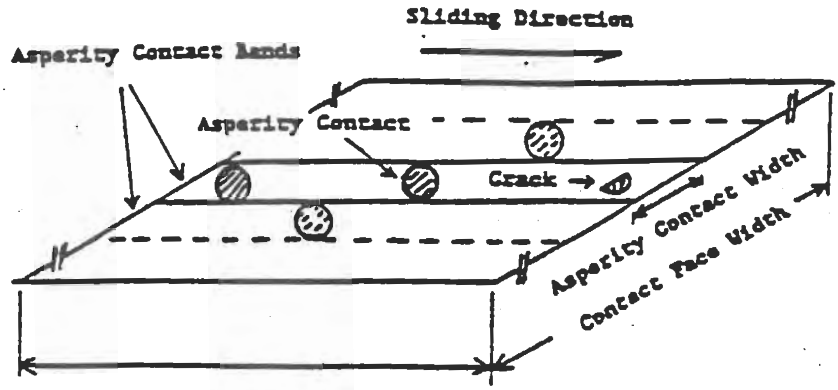

Fig. 4 Contact surface showing asperity contact band areas

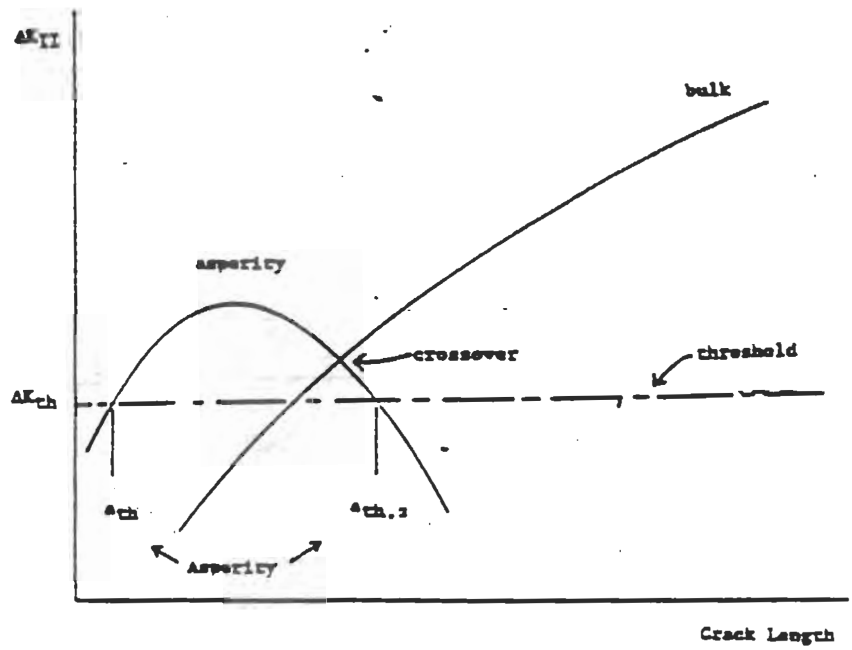

Fig. 3 Crack tip stress intensity ranges induced by asperity and bulk contact loading

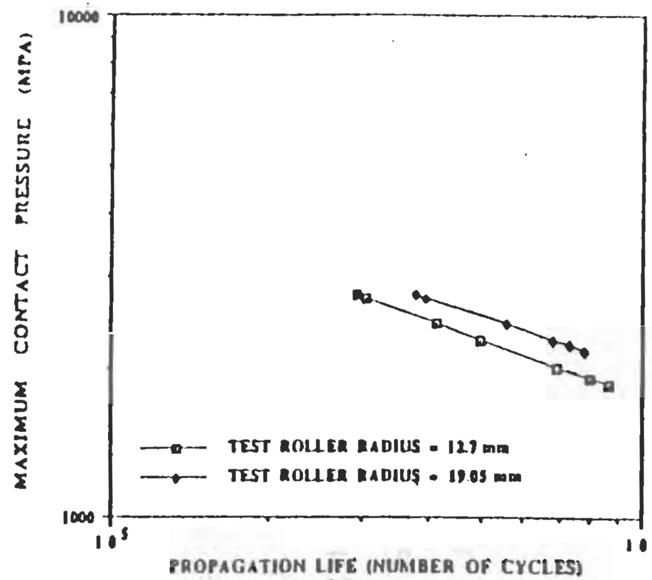

Fig. 5 Effect on predicted pitting life of varying load and contact radii

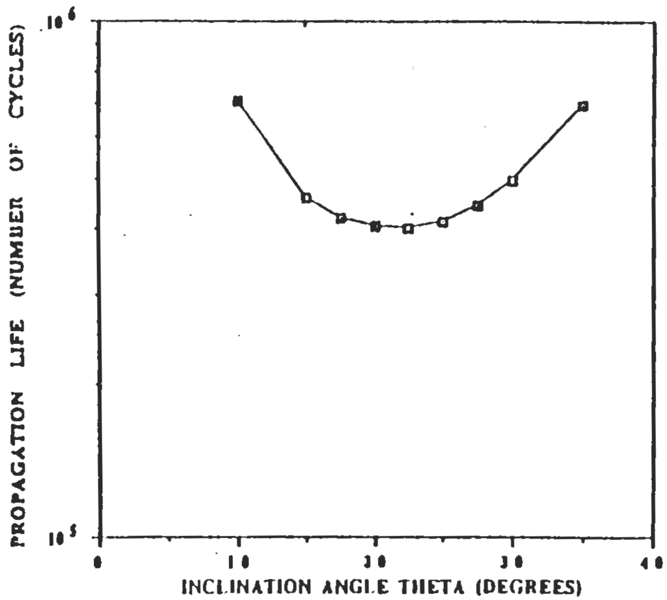

Fig. 6 Effect on predicted pitting life of changes in the crack inclination angle

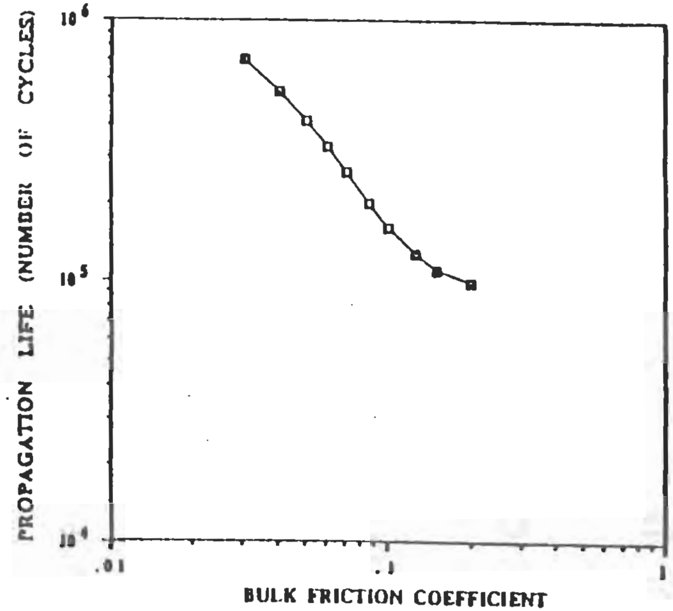

Fig. 7 Change in predicted life with variation in the bulk friction coefficient

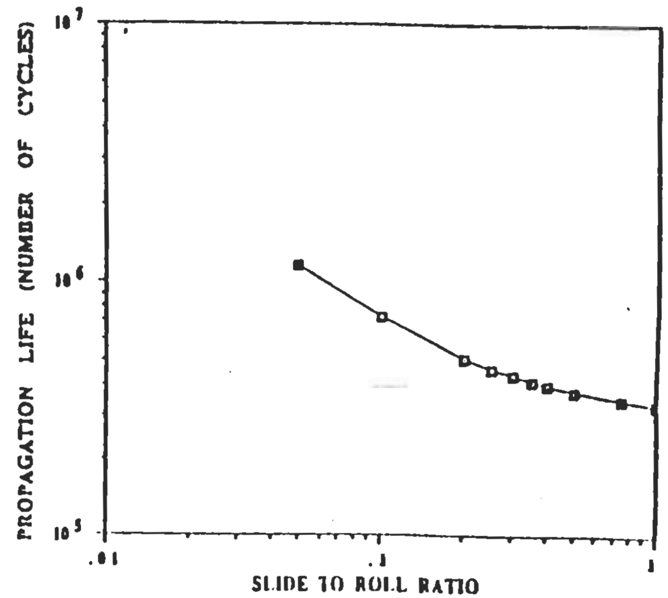

Fig. 8 Effect on predicted life of changes in the slide to roll ratio.

CONCLUDING REMARKS

- Both surface fatigue and scuffing are controlled by mixed lubrication through the average film thickness, asperity pressure, friction, and asperity temperature.

- Existing gear lubrication analyses such as TELSGE for spur gears are useful for improving predictions of surface fatigue and scuffing using current AGMA criteria with the maximum contact pressure and total temperature.

- Recent surface fatigue life model shows merit and promise leading to an improved life prediction based on fracture mechanics.

- Recent scuff experiments and modeling for rollers suggest that scuffing is generated by micro-scufing of asperities due to lubrication breakdowns leading to macro-scuffing of an extended region, and correlate with the asperity contact temperatures.